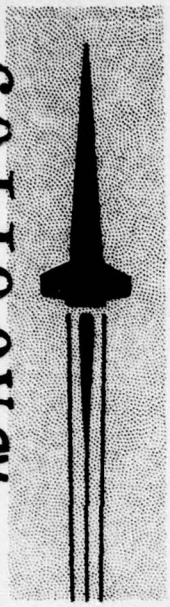



(2)

TECHNICAL REPORT T-CR-78-21

# EFFECTS OF TRANSVERSE BENDING ON THE *MOTION OF FREE-FLIGHT ROCKETS*

by

John E. Cochran, Jr.; Carl D. Evans; James B. McCurry
Aerospace Engineering Department
Auburn University
Auburn, Alabama 36830



FINAL REPORT
under
Contract DAAK40-77-C-0125

administered through

Engineering Experiment Station
Auburn University
Auburn, Alabama 36830

September 1978

U.S. ARMY MISSILE RESEARCH AND DEVELOPMENT COMMAND

Redstone Arsenal, Alabama 35809



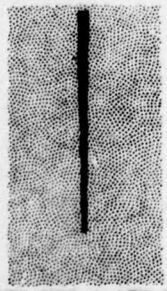

Approved for Public Release
Distribution Unlimited

## DISPOSITION INSTRUCTIONS

DESTROY THIS REPORT WHEN IT IS NO LONGER NEEDED. DO NOT RETURN IT TO THE ORIGINATOR.

## DISCLAIMER

THE FINDINGS IN THIS REPORT ARE NOT TO BE CONSTRUED AS AN OFFICIAL DEPARTMENT OF THE ARMY POSITION UNLESS SO DESIGNATED BY OTHER AUTHORIZED DOCUMENTS.

## TRADE NAMES

USE OF TRADE NAMES OR MANUFACTURERS IN THIS REPORT DOES NOT CONSTITUTE AN OFFICIAL INDORSEMENT OR APPROVAL OF THE USE OF SUCH COMMERCIAL HARDWARE OR SOFTWARE.

SECURITY CLASSIFICATION OF THIS PAGE (When Data Entered)

## REPORT DOCUMENTATION PAGE

READ INSTRUCTIONS BEFORE COMPLETING FORM

1. REPORT NUMBER: T-CR-78-21
2. GOVT ACCESSION NO.:
3. RECIPIENT'S CATALOG NUMBER:

4. TITLE (and Subtitle): EFFECTS OF TRANSVERSE BENDING ON THE MOTION OF FREE-FLIGHT ROCKETS

5. TYPE OF REPORT & PERIOD COVERED: FINAL rept. 13 June 77-30 Sep 78

6. PERFORMING ORG. REPORT NUMBER:

7. AUTHOR(s): John E. Cochran, Jr.; Cari D. Evans; James B. McCurry

8. CONTRACT OR GRANT NUMBER(s): DAAK40-77-C-0125

9. PERFORMING ORGANIZATION NAME AND ADDRESS:
Engineering Experiment Station
Auburn University
Auburn, Alabama 36830
402 958

10. PROGRAM ELEMENT, PROJECT, TASK AREA & WORK UNIT NUMBERS:

11. CONTROLLING OFFICE NAME AND ADDRESS:
Commander, US Army Missile R&D Command
Attn: DRDMI-TI
Redstone Arsenal, AL 35809

12. REPORT DATE: 29 Sep 78

13. NUMBER OF PAGES: 98

14. MONITORING AGENCY NAME & ADDRESS (if different from Controlling Office):
Commander, US Army Missile R&D Command
Attn: DRDMI-TLH
Redstone Arsenal, AL 35809

15. SECURITY CLASS. (of this report): Unclassified

15a. DECLASSIFICATION/DOWNGRADING SCHEDULE: N/A

16. DISTRIBUTION STATEMENT (of this Report):
Approved for public release; distribution unlimited

12 103 p.

17. DISTRIBUTION STATEMENT (of the abstract entered in Block 20, if different from Report)

18 DRDMI-T 19 CR-78-21

18. SUPPLEMENTARY NOTES:
The findings of this report are not to be construed as an official Department of the Army position unless so designated by other authorized documents.

19. KEY WORDS (Continue on reverse side if necessary and identify by block number):
Free-Flight Rockets
Flexible Rockets
Spinning Rockets
Mallaunch of Free Rockets
Assumed Modes

78 11 08 039

20. ABSTRACT (Continue on reverse side if necessary and identify by block number):
Two models for a transversely flexible, thrusting, free-flight rocket are presented. The first model consists of two rigid bodies connected so that relative transverse rotations of the bodies are resisted by linear restoring and damping torques. Equations of motion, both nonlinear and linear, for unconstrained motion are derived. No aerodynamic forces or moments are included in the models. Solutions to the linear equations for constant rocket spin rate are obtained in closed form and used to obtain results for a

CONT'

DD FORM 1 JAN 73 1473 EDITION OF 1 NOV 65 IS OBSOLETE
S/N 0102-LF-014-6601

CONT'

baseline rocket and parametric variations thereof. These results indicate that transverse flexibility contributes significantly to rocket mallaunch when the spin rate is high, since the long-period part of the angular rate at launch is directly proportional to spin rate and to the magnitude of transverse deformation. Effects of thrust misalignment are considered in comparing results obtained from solutions to the linear equations with flight data for a particular rocket. Equations for motion of the two-body rocket on a "rigid" (non-moving) launcher are also derived. Results obtained by numerically integrating these equations, are presented. The second and more complex model is that of a continuous, non-uniform, slender rod subject to "internal" thrust. Equations for motion on and off a "rigid" launcher are derived and converted to ordinary differential equations by using pinned-pinned-free mode shapes for the on-launch phase and free-free mode shapes for the free-flight phase. Conversion from the on-launcher equations to the free-flight equations is explained and preliminary results are discussed.

ABSTRACT

## PREFACE

This report contains a description of the work accomplished under U.S. Army Contract DAAK40-C-77-0125, during the period 13 June 1977 to 30 September 1978, for the U.S. Army Missile Research and Development Command, Redstone Arsenal, Alabama. Mr. Dean E. Christensen, the Contracting Officer's Technical Representative, was of great assistance during this effort, through both his encouragement and technical suggestions.

The authors, other than the first, contributed to the contractual effort in the following ways. Mr. Carl Evans wrote a major segment of the computer code for the continuous rocket model simulation and also worked out some of the mathematical details of the model before he had to enter the U.S. Air Force in the spring of 1978. Mr. James B. McCurry assisted in programming codes for the linearized two-body rocket model, as well as providing help on working out the two-body rocket model equations for motion on a rigid launcher. Others who made contributions are Mr. Steve Lowe, undergraduate research assistant, who performed exceptionally well as a programmer, Mr. Grant Castleberry and Mr. James Thompson, graduate research assistants, who also assisted in programming, and Mr. Gene Holloway, graduate research assistant who drew most of the figures. Finally, Mrs. Marjorie McGee deserves special recognition for her excellent typing of the manuscript.

John E. Cochran, Jr.
Project Leader

TABLE OF CONTENTS

TABLE OF CONTENTS (CONT)

LIST OF FIGURES

LIST OF FIGURES (CONT)

LIST OF TABLES

## SECTION 1. INTRODUCTION

Recently studies have been initiated[1] with the goal of improving the accuracy of free-flight rockets. Although significant reductions in dispersion of free-flight rockets have been accomplished by utilizing modern manufacturing methods, by using various techniques, such as spinning the rocket to minimize the effects of mechanical thrust misalignment,and by using launchers which provide release of the rocket without producing appreciable tipoff, further improvement in free-flight rocket accuracy will forseeably require more detailed analysis of factors which were once considered relatively insignificant. One such factor is that of transverse flexibility of the rocket.

Since no structure is perfectly rigid, all rockets are flexible to some extent. In the past, however, most free-flight rockets were designed with length to diameter (L/D) ratios less than, say, fifteen. Furthermore, the structures of these rockets tended to be dense. Such rockets are so relatively rigid that they may be modeled well as variable-mass rigid bodies.[2] Advances in materials science have, however, presented the free-rocket designer with strong, light-weight alloys and composite materials. Free-flight rockets constructed using such materials will, in general, be lighter (warhead excluded) than their predecessors and often more flexible. Furthermore, efficiency in terms of aerodynamic design dictates large L/D rockets which are now structurally possible configurations, but which tend to be more flexible than the previous rockets with smaller L/D's.

The magnitude of the effect of the flexibility of a spinning free rocket on dispersion has not been established accurately. In fact, although a good

deal of work has been expended in the area of determining the effects of flexibility on the stability and control of rockets of the launch vehicle type,[3,4,5] relatively little work concerning flexible, spinning rockets has been done. In this regard, an article by Reis and Sundberg[6] addresses the problem of aeroelastic bending of spinning sounding rockets using a simple two-rigid-body model similar to one of these discussed in the body of this report, while Womack, et. al.[7] discuss the use of a more complex model based on the use of normal modes for modeling the flexibility of such rockets. A general approach to the flexible spinning rocket problem is taken by Meriovitch.[8]

The problem treated here is different from the problem of modeling the dynamics of a flexible, spinning, sounding rocket, because in the launch of a free-flight rocket, the rocket passes from a constrained condition to a free condition. This transition is of utmost importance for free rockets, because their accuracy is greatly affected by their state at the time of release from the rocket launcher.

The primary purpose of the effort reported on here is to provide a basis for determining the effects of transverse flexibility of free-flight rockets on their motion during the launch phase and during the free-flight phase up to the time when aerodynamic reactions become significant. A two-pronged approach was adopted. On one hand, the most simple model which it was felt would give meaningful results was formulated and results obtained therefrom. Concurrently, a fairly sophisticated model, based partly on the results of Ref. 9 was developed.

The simple model of a flexible rocket consists of two rigid bodies coupled in such a way that only transverse relative rotation is allowed and that rotation is resisted by linear torsional springs (with viscous damping

also present). This model is described in Section 2. In that section, nonlinear equations of motion for the free-flight phase are derived and linear, constant-coefficient approximations to these obtained. Results obtained by solving the linear equations in closed form are presented also. Furthermore, nonlinear equations of motion for launch from a non-moving, or "rigid," launcher are derived and some results of numerical solutions to these are presented and discussed.

The more complex model is described in Section 3. This model is that of a slender, elastic body which has acting on it a thrust force and gravity (No aerodynamic reactions are considered.). Hybrid differential equations, i.e., differential equations which contain both partial and ordinary derivatives, are derived. These are replaced, approximately, with ordinary differential equations by using the method of assumed modes.[10] Two different types of mode shapes are used. For the launch phase, pinned-pinned-free mode shapes for a uniform, slender beam are used because of the desire to model the launcher (considered "rigid") constraints. For the free-flight phase, free-free mode shapes, also for a uniform, slender beam, are used. Furthermore, since instantaneous principal axes[8] are used for the free-flight phase as well as the different mode shapes, the equations needed to transform the "final conditions" of the launch phase into "initial conditions" for the free-flight phase are given also. Due to the fact that the digital computer code which is used to produce numerical solutions in both sets of equations was not completely debugged by the due date of this report, no results obtained from it are presented. However, some comments are made in regard to "anticipated" results.

In Section 4, conclusions reached during the course of this investigation are stated and recommendations for further study are made.

## SECTION 2. TWO-BODY FLEXIBLE ROCKET MODEL

### 2.1 Description of the Model

The two-body physical model of a free-flight rocket is shown in Fig. 1. The model is composed of two almost axisymmetric rigid bodies. These bodies are connected at point R in such a manner that the forward body (hereinafter called Body 2) may rotate relative to the aft body (hereinafter called Body 1) transversely with respect to the symmetry (if no dynamic imbalance is present) axis of Body 1. This relative rotation is elastically restrained and viscous damping is also present.

The point P is located at the aft end of Body 1 and the center of mass of Body 1, denoted $C_1$, is located with respect to P by the vector $\underline{r}_1$. The vector $\underline{\ell}_1$ connects the points P and R and the vectors $\underline{r}_2$ and $\underline{\ell}_2$ are directed from R to $C_2$ (the center of mass of Body 2) and from $C_2$ to Q, respectively. The points P and Q correspond to the points at which the rocket is supported while it is on the launcher.

During the launch phase, it is assumed that the launcher does not move. Hence, it is referred to as a "rigid" launcher. Thus, while on the launcher, the rocket is constrained so that the points P and Q translate along a fixed straight line. In addition to the constraint forces acting at P and Q, the rocket is subjected to external forces due to thrust and gravity while it is on the launcher. However, its mass is assumed constant during this phase.

During the free-flight phase, a free-flight rocket is generally acted on by gravity, aerodynamic reactions and forces and moments due to the flow internal to the rocket. At present, it is desired to maintain simplicity in our model.

Hence, the aerodynamic reactions as well as all the forces and moments on the rocket due to internal flow, except the thrust, are neglected. These should be relatively small compared to the thrust and weight during the first two or three tenths of a second of flight. The thrust force is assumed to act only on Body 1 and its magnitude and direction relative to the longitudinal axis of Body 1 are assumed constant. Furthermore, the mass of the rocket is assumed constant during this phase as in the launch phase. The assumption of constant mass should be fairly valid for the time period immediately after launch during which optical lever data is acquired.

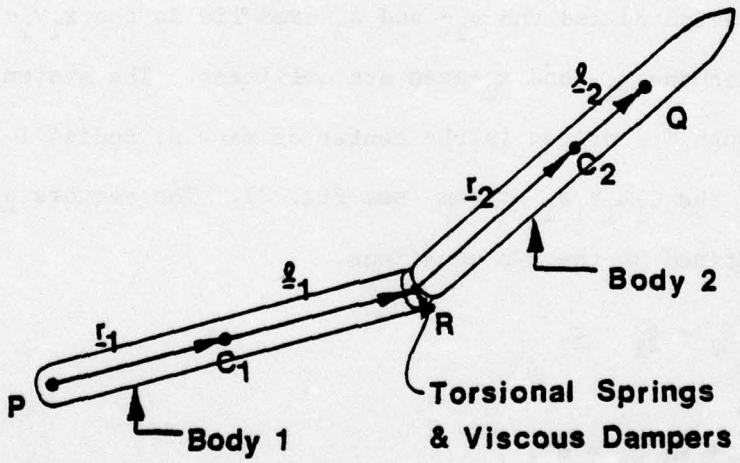


Figure 1. Simple two-body rocket model.

## 2.2 Nonlinear Equations for the Free-Flight Phase

The equations of motion for the physical model described for the off-the-launcher, or free-flight phase,[†] may be obtained by applying Newton's laws of motion directly, or by using an energy-based method such as Lagrange's. Here we choose the direct approach in the sense of Ref. 2. Equations of motion for the system of two bodies are first obtained. Next, the equations of motion for Body 2 are derived.

### Explanation of Notation

A dextral, orthogonal, coordinate system, OXYZ, fixed to the earth's surface is used as the reference for all motion. A Body 1-fixed coordinate system, $C_1x_1y_1z_1$, and a corresponding Body 2-fixed system, $C_2x_2y_2z_2$, are defined such that the $x_j$-axis is the longitudinal axis of Body j. The $y_1$- and $z_1$-axes are arbitrarily oriented and the $y_2$- and $z_2$-axes lie in the $x_1y_1$- and $x_1z_1$-planes, respectively, when the $x_1$- and $x_2$-axes are collinear. The system Cxyz is defined such that, although its origin is the center of mass of Bodies 1 and 2, its axes are aligned with the $C_1x_1y_1z_1$ system (see Fig. 2). The vectors $\underline{\rho}_1$ and $\underline{\rho}_2$ shown in Fig. 2 are defined by the two equations,

$$\underline{\rho}_2 - \underline{\rho}_2 = \underline{\ell}_1 + \underline{r}_2 \tag{1}$$

and

$$m_1 \underline{\rho}_1 + m_2 \underline{\rho}_2 = \underline{0} \ , \tag{2}$$

where $m_j$ is the mass of Body j. Thus,

$$\underline{\rho}_1 = -\mu(\underline{\ell}_1 + \underline{r}_2) \tag{3a}$$

---

[†]The free-flight phase is considered first in this report because it was considered first in time during this contractual effort.

and

$$\underline{\rho}_2 = (1-\mu)(\underline{\ell}_1+\underline{r}_2) \tag{3b}$$

where $\mu = m_2/M$, with $M = m_1 + m_2$ denoting the total mass of the rocket.

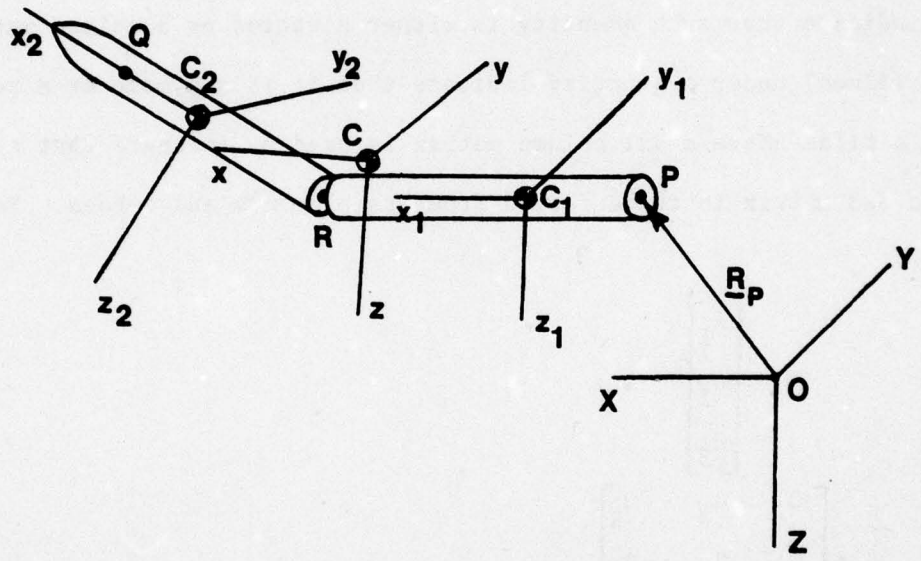


Figure 2. Coordinate systems used in two-body model analysis.

In what follows, the angular velocity of the Cxyz coordinate system (and also the $C_1x_1y_1z_1$ system) is $\underline{\Omega}$, the angular velocity of the $Cx_2y_2z_2$ system is $\underline{\omega}_2$ and the angular velocity of the $C_2x_2y_2z_2$ system relative to the cxyz system is $\underline{\omega}_{2/1}$, Also, the centroidal inertia dyadic of Body j is $\underline{\underline{I}}_j$.

In addition to the notation thus far defined, we shall use a dot over a matrix, or a vector, to denote total differentiation of that quantity with respect to time, while a small circle over a vector will be used to denote differentiation with respect to time of only the components of that vector as resolved in the Cxyz system. Furthermore, the notation $\delta\underline{V}/\delta t$ is used to denote the derivative of the components of a vector quantity $\underline{V}$ as resolved in the $C_2x_2y_2z_2$ coordinate frame. A bar (line) under a quantity is used to indicate that such quantity is either a vector or a column matrix, while two bars (lines) under a quantity indicate that it is a dyadic or a square matrix. Finally, a tilde above a 3x1 column matrix is used to indicate that a skew-symmetric 3x3 matrix is to be formed from its elements and zeroes. For example, given

$$\underline{\Omega} = \begin{bmatrix} \Omega_1 \\ \Omega_2 \\ \Omega_3 \end{bmatrix} , \tag{4}$$

$$\underline{\underline{\tilde{\Omega}}} \triangleq \begin{bmatrix} 0 & -\Omega_3 & \Omega_2 \\ \Omega_3 & 0 & -\Omega_1 \\ -\Omega_2 & \Omega_1 & 0 \end{bmatrix} . \tag{5}$$

Equations of Motion for the System

Newton's laws of motion for a particle may be used to show that the time rate of change of the angular momentum of the system composed of Bodies 1 and 2 about C is equal to $\underline{T}_c$, the external torque about C. The angular momentum of the system about C, $\underline{H}_c$, may be expressed in the form,

$$\underline{H}_c = \underline{\underline{I}}_1 \cdot \underline{\Omega} + \underline{\underline{I}}_2 \cdot(\underline{\Omega} + \underline{\omega}_{2/1}) + m_1 \underline{\rho}_1 \times \dot{\underline{\rho}}_1 + m_2 \underline{\rho}_2 \times \dot{\underline{\rho}}_2 \,. \tag{6}$$

By using Eqs. (3), we may rewrite $\underline{H}_c$ as

$$\underline{H}_c = \underline{\underline{I}}_1 \cdot \underline{\Omega} + \underline{\underline{I}}_2 \cdot(\underline{\Omega} + \underline{\omega}_{2/1}) + \sigma(\underline{\ell}_1 + \underline{r}_2)\times(\dot{\underline{\ell}}_1 + \dot{\underline{r}}_2), \tag{7}$$

where $\sigma = m_1 m_2/M$. Since $\dot{\underline{H}}_c = \underline{T}_c$, it follows from Eq. (7) that

$$\underline{T}_c = \underline{\underline{I}}_1 \cdot \mathring{\underline{\Omega}} + \underline{\Omega} \times \underline{\underline{I}}_1 \cdot \underline{\Omega} + \underline{\underline{I}}_2 \cdot(\delta\underline{\Omega}/\delta t + \delta\underline{\omega}_{2/1}/\delta t) + (\underline{\Omega} + \underline{\omega}_{2/1}) \times \underline{\underline{I}}_2 \cdot(\underline{\Omega} + \underline{\omega}_{2/1}) + \sigma(\underline{\ell}_1 + \underline{r}_2) \times (\ddot{\underline{\ell}}_1 + \ddot{\underline{r}}_2) \,. \tag{8}$$

The right-hand side of Eq. (8) is actually more complicated than it might first appear, because $\ddot{\underline{\ell}}_1$ and $\ddot{\underline{r}}_2$ are rather complicated expressions when expanded out in full.

It is convenient to convert Eq. (8) into its matrix counterpart at this point. If we use the unit vectors $\hat{\underline{i}}$, $\hat{\underline{j}}$ and $\hat{\underline{k}}$ (which are parallel to the x-, y- and z-axes, respectively) as our basis vectors (Body 1 basis) for writing the matrix equation and want to express $\underline{\omega}_{2/1}$, $\underline{\underline{I}}_2$ and $\underline{r}_2$ in the Body 2 basis (unit vectors $\hat{\underline{i}}_2$, $\hat{\underline{j}}_2$ and $\hat{\underline{k}}_2$), we need a transformation matrix to relate the two bases. A suitable matrix is

$$\underline{\underline{A}} = \begin{bmatrix} c\theta_2 c\theta_3 & c\theta_2 s\theta_3 & -s\theta_2 \\ -s\theta_3 & c\theta_3 & 0 \\ c\theta_3 s\theta_2 & -s\theta_2 s\theta_3 & c\theta_2 \end{bmatrix}, \tag{9}$$

where $\theta_2$ and $\theta_3$ (see Fig. 3) are angles of relative rotation of Body 2 with respect to Body 1 about the $y_2$- and $z_1$-axes, respectively, and $c\theta \triangleq \cos\theta$ and $s\theta \triangleq \sin\theta$. The matrix $\underline{\underline{A}}$ thus relates the unit vector triads $(\hat{\underline{i}}, \hat{\underline{j}}, \hat{\underline{k}})$ and $(\underline{i}_2, \underline{j}_2, \underline{k}_2)$ through the equation,

$$\begin{bmatrix} \hat{\underline{i}}_2 \\ \hat{\underline{j}}_2 \\ \hat{\underline{k}}_2 \end{bmatrix} = \underline{\underline{A}} \begin{bmatrix} \hat{\underline{i}} \\ \hat{\underline{j}} \\ \hat{\underline{k}} \end{bmatrix} . \tag{10}$$

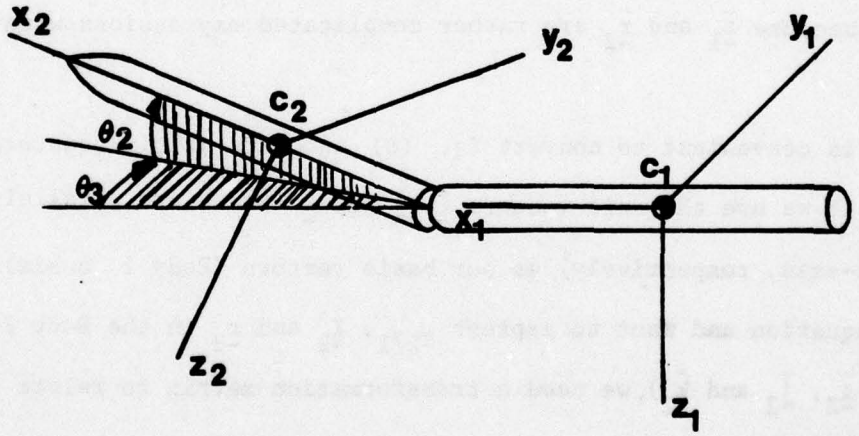


Figure 3. Relative orientation of bodies 1 and 2.

It can be shown that

$$\dot{\underline{\underline{A}}} = -\tilde{\underline{\omega}}_{2/1}\,\underline{\underline{A}}\,, \tag{11}$$

and, since (a number under a matrix denotes the basis used)

$$\underline{\Omega}_2 = \underline{\underline{A}}\,\underline{\Omega}_1\,,$$

the <u>matrix</u> counterpart of the <u>vector</u> $\delta\underline{\Omega}/\delta t$ is $-\tilde{\underline{\omega}}_{2/1}\,\underline{\underline{A}}\,\underline{\Omega}_1 + \underline{\underline{A}}\,\dot{\underline{\Omega}}$. This fact may be used to get the results,*

$$\begin{aligned}
\underline{T}_c = {} & \underline{\underline{I}}\,\dot{\underline{\Omega}} + \tilde{\underline{\Omega}}\,\underline{\underline{I}}\,\underline{\Omega} + \underline{\underline{A}}^T\,\underline{\underline{I}}_2(\underline{\underline{A}}\,\dot{\underline{\Omega}} - \tilde{\underline{\omega}}_{2/1}\,\underline{\underline{A}}\,\underline{\Omega} + \dot{\underline{\omega}}_{2/1}) \\
& + (\tilde{\underline{\Omega}}\,\underline{\underline{A}}^T + \underline{\underline{A}}^T\,\tilde{\underline{\omega}}_{2/1})\,\underline{\underline{I}}_2\,(\underline{\underline{A}}\,\underline{\Omega} + \underline{\omega}_{2/1}) \\
& + \sigma(\tilde{\underline{\ell}}_1 + \underline{\underline{A}}^T\,\underline{r}_2\,\underline{\underline{A}})\,[-\tilde{\underline{\ell}}_1\,\dot{\underline{\Omega}} + \tilde{\underline{\Omega}}\,\tilde{\underline{\Omega}}\,\underline{\ell}_1 \\
& - \underline{\underline{A}}^T\,\tilde{\underline{r}}_2\,(\underline{\underline{A}}\,\dot{\underline{\Omega}} - \tilde{\underline{\omega}}_{2/1}\,\underline{\underline{A}}\,\underline{\Omega} + \dot{\underline{\omega}}_{2/1}) \\
& + (\tilde{\underline{\Omega}} + \underline{\underline{A}}^T\,\tilde{\underline{\omega}}_{2/1}\,\underline{\underline{A}})(\tilde{\underline{\Omega}} + \underline{\underline{A}}^T\,\tilde{\underline{\omega}}_{2/1}\,\underline{\underline{A}})\underline{\underline{A}}^T\,\underline{r}_2]\,,
\end{aligned} \tag{13}$$

where the Body 1 basis is used unless otherwise indicated. Also

$$\underline{T}_{1c} = -[\mu(\tilde{\underline{\ell}}_1 + \underline{\underline{A}}^T\,\tilde{\underline{r}}_2\,\underline{\underline{A}}) + \tilde{\underline{r}}_1]\underline{F}_{1T}, \tag{14}$$

where $\underline{F}_T$ is the thrust.

Equation (13) governs the motion of the system of two bodies about the system center of mass. It can be considered an equation from which $\underline{\Omega}_1$ may be obtained. An additional, independent, matrix, differential equation for $\underline{\omega}_{2/1}$ is needed.

*A superscript T is used to denote the transpose of a matrix.

Relative Motion of Body 2

A differential equation governing the motion of Body 2 with respect to Body 1 may be obtained by using the fact that the time rate of change of the angular momentum of Body 2 about R, minus the mass of Body 2 times the cross product of $\underline{r}_2$ and the acceleration of the point R, is equal to the torque about R. To see that this is the case, we write $\underline{a}_{dm_2}$, the acceleration of $dm_2$ (an element of mass of Body 2) in the form,

$$\underline{a}_{dm_2} = \ddot{\underline{R}}_p + \ddot{\underline{r}}_1 + \ddot{\underline{\ell}}_1 + \ddot{\underline{r}}_2 + \ddot{\underline{\rho}}^*_2 \ , \tag{15}$$

where $\underline{\rho}^*_2$ is a generic position vector from $C_2$ to $dm_2$. By forming the cross product of $\underline{r}_2 + \underline{\rho}^*_2$ with each side of Eq. (15) and integrating over the mass of Body 2, we get[†]

$$m_2 \, \underline{r}_2 \times (\ddot{\underline{R}} + \ddot{\underline{r}}_1 + \ddot{\underline{\ell}}_1) + m_2 \, \underline{r}_2 \times \ddot{\underline{r}}_2$$

$$+ \int_{m_2} \underline{\rho}^*_2 \times \ddot{\underline{\rho}}^*_2 \, dm_2 = \int_{m_2} (\underline{r}_2 + \underline{\rho}^*_2) \times \underline{a}_{dm_2} \, dm_2 \ . \tag{16}$$

But,

$$\int_{m_2} (\underline{r}_2 + \underline{\rho}^*_2) \times \underline{a}_{dm_2} \, dm_2 = \underline{T}_R, \text{ the torque on Body 2 about R,} \tag{17}$$

and the sum of the second and third terms on the left-hand side of Eq. (16) is the time rate of change of the angular momentum of Body 2 due to its <u>rotation</u> about the point R. Also, the acceleration of R is $\ddot{\underline{R}}_p + \ddot{\underline{r}}_1 + \ddot{\underline{\ell}}_1$.

Now, we first introduce the centroidal inertia dyadic of Body 2 and the equation for translational motion of $m_2$,

---

[†]Note that $\int_{m_2} \underline{\rho}^*_2 \, dm_2 \equiv \underline{0}$, by virtue of the definition of $\underline{\rho}^*_2$.

$$\ddot{\underline{R}}_p + \ddot{\underline{r}}_1 + \mu(\ddot{\underline{r}}_2 + \ddot{\underline{\ell}}_1) = \underline{F}/M, \tag{18}$$

where $\underline{F}$ is the external force on the rocket, into Eq. (16). Next, using $M\underline{g}$ as the force due to gravity on the two-body system and $F_T$ as the thrust, $\underline{F}=\underline{F}_T + M\underline{g}$ and $\underline{T}_R=\underline{T}_{2/1} + \mu\, \underline{r}_2 \times \underline{F}_T$, where $\underline{T}_{2/1}$ is the torque on Body 2 due to Body 1, we get

$$\begin{aligned}\underline{T}_{2/1} = {} & \mu\, \underline{r}_2 \times \underline{F}_T + \sigma\, \underline{r}_2 \times(\ddot{\underline{\ell}}_1 + \ddot{\underline{r}}_2) \\ & + \underline{\underline{I}}_2 \cdot (\delta\underline{\Omega}/\delta t + \delta\underline{\omega}_{2/1}/\delta t) \\ & + (\underline{\Omega} + \underline{\omega}_{2/1}) \times \underline{\underline{I}}_2 \cdot (\underline{\Omega} + \underline{\omega}_{2/1}).\end{aligned} \tag{19}$$

The Body 1-basis, matrix counterpart of Eq. (18) is

$$\begin{aligned}\underline{T}_{2/1} = {} & \mu\, \underline{\underline{A}}^T \tilde{\underline{r}}_2\, \underline{\underline{A}}\, \underline{F}_T + \underline{\underline{A}}^T[\underline{\underline{I}}_2 - \sigma\, \tilde{\underline{r}}_2\, \underline{\underline{A}}\, \underline{\ell}_1 - \sigma\, \tilde{\underline{r}}_2\, \tilde{\underline{r}}_2]\, \underline{\underline{A}}\, \dot{\underline{\Omega}} \\ & + \underline{\underline{A}}^T[\underline{\underline{I}}_2 - \sigma\, \tilde{\underline{r}}_2\, \tilde{\underline{r}}_2]\, \dot{\underline{\omega}}_{2/1} \\ & + \sigma\, \underline{\underline{A}}^T\, \tilde{\underline{r}}_2[\underline{\underline{A}}\, \tilde{\underline{\Omega}}\, \tilde{\underline{\Omega}}\, \underline{\ell}_1 + \tilde{\underline{r}}_2\, \tilde{\underline{\omega}}_{2/1}\, \underline{\underline{A}}\, \underline{\Omega} \\ & + (\tilde{\underline{\Omega}} + \underline{\underline{A}}^T\, \tilde{\underline{\omega}}_{2/1}\, \underline{\underline{A}})(\tilde{\underline{\Omega}} + \underline{\underline{A}}^T\, \tilde{\underline{\omega}}_{2/1}\, \underline{\underline{A}})\underline{\underline{A}}^T\, \underline{r}_2] \\ & - \underline{\underline{A}}^T\, \underline{\underline{I}}_2\, \tilde{\underline{\omega}}_{2/1}\, \underline{\underline{A}}\, \underline{\Omega} + \tilde{\underline{\Omega}}\, \underline{\underline{A}}^T\, \underline{\underline{I}}_2\, \underline{\underline{A}}\, \underline{\Omega} + \underline{\underline{A}}^T\tilde{\underline{\omega}}_{-2/1}\, \underline{\underline{I}}_2\, \underline{\underline{A}}\, \underline{\Omega} \\ & + \tilde{\underline{\Omega}}\, \underline{\underline{A}}^T\, \underline{\underline{I}}_2\, \underline{\omega}_{2/1} + \underline{\underline{A}}^T\, \tilde{\underline{\omega}}_{2/1}\, \underline{\underline{I}}_2\, \underline{\omega}_{2/1},\end{aligned} \tag{20}$$

where $\underline{F}_T$, $\underline{\ell}_1$ and $\underline{\Omega}$ are expressed in the Body 1 basis and $\underline{r}_2$, $\underline{\underline{I}}_2$ and $\underline{\omega}_{2/1}$ are expressed in the Body 2 basis. Equation (20) is the desired matrix equation which, along with Eq. (13), governs the attitude motion of the rocket's <u>two parts</u>.

We can rewrite Eq. (20) in the form,

$$\underline{\underline{J}}_{21}\,\dot{\underline{\Omega}} + \underline{\underline{J}}_{22}\,\dot{\underline{\omega}}_{2/1} = \underline{T}_2 \ , \tag{21}$$

where the definitions of $\underline{\underline{J}}_{22}$, $\underline{\underline{J}}_{12}$ and $\underline{T}_2$ follow from Eq. (19). Then[†]

$$\dot{\underline{\omega}}_{2/1} = \underline{\underline{J}}_{22}^{-1}\,\underline{T}_2 - \underline{\underline{J}}_{22}^{-1}\,\underline{\underline{J}}_{22}\,\dot{\underline{\Omega}} \ . \tag{22}$$

In a similar manner, Eq. (13) can be rewritten in the form,

$$\underline{\underline{J}}_{11}\,\dot{\underline{\Omega}} + \underline{\underline{J}}_{12}\,\dot{\underline{\omega}}_{2/1} = \underline{T}_1 \ . \tag{23}$$

Thus, by using Eq. (22) to eliminate $\dot{\underline{\omega}}_{2/1}$ from Eq. (23), we get

$$[\underline{\underline{J}}_{11} - \underline{\underline{J}}_{12}\,\underline{\underline{J}}_{22}^{-1}\,\underline{\underline{J}}_{21}]\,\dot{\underline{\Omega}} = \underline{T}_1 - \underline{\underline{J}}_{12}\,\underline{\underline{J}}_{22}^{-1}\,\underline{T}_2 \ . \tag{24}$$

Similarly, by solving Eq. (23) for $\dot{\underline{\Omega}}$ and using that solution in Eq. (21), we obtain

$$[\underline{\underline{J}}_{22} - \underline{\underline{J}}_{22}\,\underline{\underline{J}}_{11}^{-1}\,\underline{\underline{J}}_{12}]\,\dot{\underline{\omega}}_{2/1} = \underline{T}_2 - \underline{\underline{J}}_{22}\,\underline{\underline{J}}_{11}^{-1}\,\underline{T}_1 \ . \tag{25}$$

The derivatives $\dot{\underline{\Omega}}$ and $\dot{\underline{\omega}}_{2/1}$ can be obtained from Eqs. (24) and (25) by simply inverting the 3x3 matrices in square brackets and premultiplying each equation by the proper inverse matrix.

Kinematic Equations for Rotation

The orientation of the Cxyz coordinate frame is defined by the Euler angles $\Psi$, $\Theta$, and $\Phi$. As shown in Fig. 4, a 3-2-1 rotation sequence is used. The kinematic equations for these angles are

$$\dot{\Psi} = (\Omega_2 \sin \Phi + \Omega_3 \cos \Phi)/\cos \Theta, \tag{26a}$$

[†]A superscript -1 is used to denote the inverse of a square matrix.

$$\dot{\Theta} = \Omega_2 \cos \Phi - \Omega_3 \sin \Phi \tag{26b}$$

and

$$\dot{\Phi} = \Omega_1 + (\Omega_2 \sin \Phi + \Omega_3 \cos \Phi)\tan \Theta, \tag{26c}$$

where the $\Omega_j$, j=1,2,3, are the elements of $\underline{\Omega}$.
$\underline{1}$

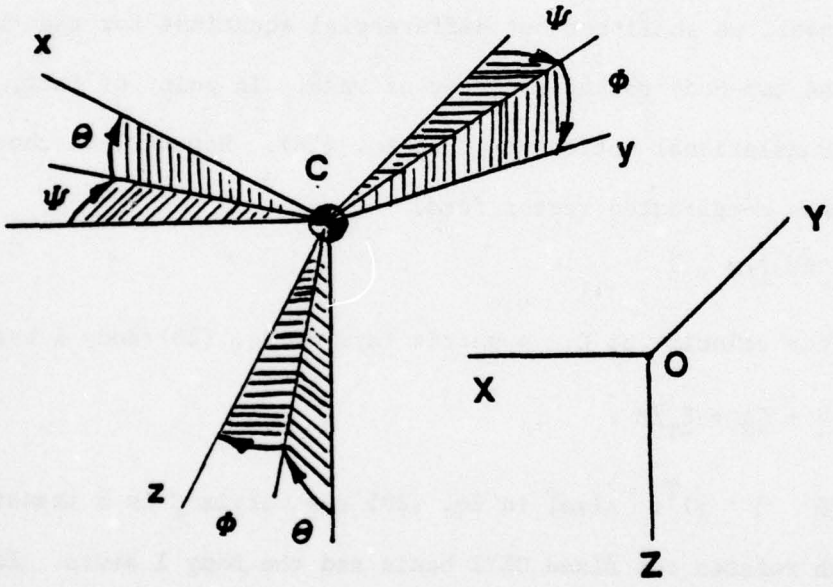


Figure 4. Orientation of body 1.

The orientation of Body 2 relative to Body 1 is defined by the previously introduced angles $\theta_2$ and $\theta_3$. These angles are used in a 3-2 rotation sequence, as shown in Fig. 3. From the geometry on Fig. 3, one may deduce the kinematic equations,

$$\dot{\theta}_3 = \omega_3/\cos\,\theta_2 \tag{27a}$$

$$\dot{\theta}_2 = \omega_2 \ , \tag{27b}$$

from which these angles may be determined. Here, $\omega_2$ and $\omega_3$ are elements of $\underline{\omega}_{2/1}$, i.e., $\underline{\omega}_{2/1} = (0 \quad \omega_2 \quad \omega_3)^T$ .

Translational Motion

Although it is of secondary importance in this investigation, for the sake of completeness, we shall set out differential equations for the translational motion of the two-body rocket's center of mass. In point of fact, the equation governing translational motions of C is Eq. (18). However, we chose to write it in the less complicated vector form,

$$\overset{\circ}{\underline{V}} = -\ \underline{\Omega} \times \underline{V} + \underline{F}/M \ , \tag{28}$$

where $\underline{V}$ is the velocity of C. A matrix form of Eq. (28)(Body 1 basis) is

$$\dot{\underline{V}} = \tilde{\underline{\Omega}}\ \underline{V} + \underline{\underline{C}}\,\underline{g} + \underline{F}_T/M \ , \tag{29}$$

where $\underline{g} = (0 \quad 0 \quad g)^T$. Also, in Eq. (29) the matrix $\underline{\underline{C}}$ is a transformation matrix which relates the fixed OXYZ basis and the Body 1 basis. Explicitly,

$$\underline{\underline{C}} = \begin{bmatrix} c\Theta c\Psi & c\Theta s\Psi & -s\Theta \\ -c\Phi s\Psi + s\Phi c\Psi s\Theta & c\Phi c\Psi + s\Phi s\Psi s\Theta & s\Phi c\Theta \\ s\Phi s\Psi + c\Phi c\Psi \sin\Theta & -s\Phi c\Psi + c\Phi s\Psi s\Theta & c\Phi c\Theta \end{bmatrix} \ . \tag{30}$$

Furthermore, $\underline{V} = (u \quad v \quad w)^T$. Notice that, although the values of $\dot{\underline{R}}_p$, $\dot{\underline{r}}_1$, $\dot{\underline{\ell}}_1$ and $\dot{\underline{r}}_2$ at the instant of release of the rocket from the launcher are

needed to define u, v and w at that point in time, thereafter, they may be determined by solving Eq. (29).

The matrix kinematic equation for translational motion is simply

$$\begin{bmatrix} \dot{X} \\ \dot{Y} \\ \dot{Z} \end{bmatrix} = \underline{\underline{C}}^T \begin{bmatrix} u \\ v \\ w \end{bmatrix} . \tag{31}$$

The nonlinear equations for motion of the two-body rocket model during the free-flight phase consist of Eqs. (24), (25), (26), (27), (29), and (31). These equations are complicated and a closed-form,general solution to them does not appear attainable. However, several reasonable assumptions may be made which allow us to simplify the equations greatly, thereby obtaining equations to which closed-form solutions may be obtained. The next subsection contains the details of these simplifications.

## 2.3 Linear Equations for the Free-Flight Phase

The equations derived in the previous subsection may be greatly simplified by making several assumptions which, generally, are reasonable ones. The first of these is that the angles $\theta_2$ and $\theta_3$, which in effect are measures of the amount the rocket bends, are small enough that $\sin \theta_2 \simeq \theta_2$, $\cos \theta_2 \simeq 1$, $\sin \theta_3 \simeq \theta_3$, and $\cos \theta_3 \simeq 1$. By adopting this assumption, we may use the approximation,

$$\underline{A} \simeq \begin{bmatrix} 1 & \theta_3 & -\theta_2 \\ -\theta_3 & 1 & 0 \\ \theta_2 & 0 & 1 \end{bmatrix} , \tag{32}$$

for the transformation matrix $\underline{A}$ and also may approximate Eq. (27a) with

$$\dot{\theta}_3 \simeq \omega_3 . \tag{33}$$

Our second assumption is that the angles $\Theta$ and $\Psi$ are also small enough that the sines of these angles are approximately equal to the angles in radians and that the cosines of the angles are each approximately unity. The assumption that $\Theta$ is small limits the launcher elevation to small angles. However, at small values of $\Theta$, the effects of bending of the rocket due to its weight will be greatest, so that this is a conservative assumption.

With small $\Theta$ and $\Psi$, we get the following approximation to $\underline{C}$:

$$\underline{C} \simeq \begin{bmatrix} 1 & \Psi & -\Theta \\ -\Psi c\Phi + \Theta s\Phi & c\Phi & s\Phi \\ \Psi s\Phi + \Theta c\Phi & -s\Phi & c\Phi \end{bmatrix} . \tag{34}$$

We also may simplify Eqs. (26) to get

$$\dot{\Psi} \simeq \Omega_2 \, s\Phi + \Omega_3 \, c\Phi, \tag{35a}$$

$$\dot{\Theta} \simeq \Omega_2 \, c\Phi - \Omega_3 \, s\Phi \tag{35b}$$

and

$$\dot{\Phi} \simeq \Omega_1 + \dot{\Psi} \, \Theta . \tag{35c}$$

Now, if $\Psi$ and $\Theta$ are to remain small, $\dot{\Psi}$ and $\dot{\Theta}$ must be small. Furthermore, for a "good" launch, $\dot{\Psi}$ and $\dot{\Theta}$ <u>are</u> small compared to one radian per second. It

then follows, from Eqs. (35), that $\Omega_2$ and $\Omega_3$ are of the same magnitude as $\dot{\Theta}$ and $\dot{\Psi}$ and hence are "small."

We shall further assume that $\Omega_1 >> \dot{\Psi}\,\Theta$. Thus, Eq. (35c) can be further simplified to get the approximate equation,

$$\dot{\Phi} \simeq \Omega_1 \ . \tag{36}$$

The assumption that $\dot{\Psi}$ and $\dot{\Theta}$ are small compared to unity makes it possible for us to simplify the equations of rotational motion significantly. First of all, we can discard any products of $\Omega_2$ and $\Omega_3$, and also any squares of these variables, from the equations. Furthermore, it generally is possible to assume that $\omega_2$ and $\omega_3$ are also less than unity, although for large-amplitude, high-frequency vibration they may have magnitudes near unity at times.† Thus, any products of $\omega_2$ and $\omega_3$ or of $\omega_2$ and $\omega_3$ and $\Omega_2$ or $\Omega_3$ may be discarded as being higher order.

The terms which contain $\Omega_1^2$ and $\dot{\Omega}_1$ are retained for the present. These may be very large compared to unity if the rocket is spinning.

Although more generality could be maintained with additional effort, it is assumed here that the following geometric equations hold:

$$\underline{r}_1 = (r_1 \quad 0 \quad 0)^T \ , \tag{37a}$$

$$\underline{\ell}_1 = (\ell_1 \quad 0 \quad 0)^T \tag{37b}$$

and

$$\underline{r}_2 = (r_2 \quad 0 \quad 0)^T \ , \tag{37c}$$

where $r_1$, $\ell_1$ and $r_2$ are constants. These equations imply that the centers of mass of the bodies both lie on the x-axis when the rocket is not "bent."

†Generally, lower amplitudes are associated with higher frequencies.

The inertia matrices are assumed to have the forms,

$$\underline{\underline{I}}_1 = \begin{bmatrix} A_1 & 0 & 0 \\ 0 & A_2 & 0 \\ 0 & 0 & A_2 \end{bmatrix} \tag{38}$$

and

$$\underline{\underline{I}}_2 = \begin{bmatrix} B_1 & 0 & 0 \\ 0 & B_2 & 0 \\ 0 & 0 & B_2 \end{bmatrix}, \tag{39}$$

which of course imply that the bodies are axisymmetric and dynamically balanced. The torque $\underline{T}_{2/1}$ is considered to be a linear function of $\dot{\theta}_2$, $\dot{\theta}_3$, $\theta_2$ and $\theta_3$ and $\underline{F}_T = (F_T \quad \alpha_z F_T \quad -\alpha_y F_T)^T$, where $\alpha_y$ and $\alpha_z$ are small mechanical thrust misalignment angles as shown in Fig. 5.

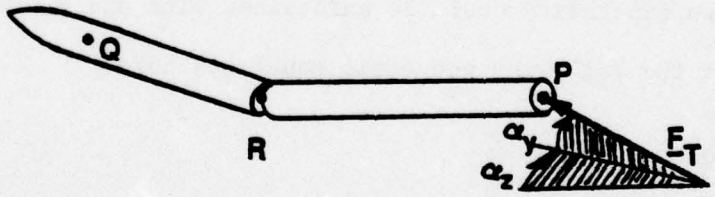


Figure 5. Mechanical thrust misalignment angles.

After a good deal of algebra and the use of the above stated assumptions, the equations of rotational motion may be reduced to the forms,

$$\dot{\Omega}_1 = T_s / I_A \tag{40}$$

and

$$\underline{\underline{I}}\,\dot{\underline{x}} = \underline{\underline{B}}\,\underline{x} + \underline{T}, \tag{41}$$

where $T_s$ is the x-component of the torque $\underline{T}_c$ and $I_A = A_1 + B_1$ is the moment of inertia about the x-axis when there is no deformation of the rocket. In Eq. (41), $\underline{\underline{I}}$ is a 6x6 matrix, the nonzero elements of which are $I_{11} = A_2+B_2 + \sigma(\ell_1+r_2)^2$, $I_{13} = B_2 + \sigma r_2(\ell_1+r_2)$, $I_{22} = I_{11}$, $I_{42} = I_{24} = I_{31} = I_{13}$, $I_{33} = I_{44} = B_2 + \sigma r_2^2$ and $I_{55} = I_{66} = 1$. Furthermore, $\underline{x} = (\Omega_2\ \Omega_3\ \omega_2\ \omega_3\ \theta_2\ \theta_3)^T$ and the nonzero elements of the 6x6 matrix $\underline{\underline{B}}$ are

$$\begin{aligned}
B_{12} &= \Omega_1[A_2 + B_2 + \sigma(\ell_1+r_2)^2 - A_1-B_1] ,\\
B_{14} &= \Omega_1[2B_2-B_1 + 2\,\sigma\, r_2(\ell_1+r_2)],\\
B_{15} &= \mu r_2 F_T + \Omega_1^2[B_2-B_1 + \sigma r_2(\ell_1+r_2)]\\
B_{16} &= \dot{\Omega}_1[B_2 - B_1 + \sigma r_2(\ell_1+r_2)]\\
B_{21} &= - B_{12},\\
B_{23} &= - B_{14},\\
B_{25} &= - B_{16},\\
B_{26} &= B_{15},\\
B_{32} &= \Omega_1[B_2-B_1 + \sigma r_2(\ell_1+r_2)]\\
B_{33} &= -c,\\
B_{34} &= \Omega_1[2\,B_2-B_1 + 2\sigma r_2^2] ,\\
B_{35} &= \mu r_2 F_T + \Omega_1^2[B_2-B_1 + \sigma r_2^2] -k,\\
B_{36} &= \dot{\Omega}_1[B_2-B_1 + \sigma r_2^2]
\end{aligned} \tag{42}$$

$$B_{41} = - B_{32},$$

$$B_{43} = - B_{34},$$

$$B_{44} = - c,$$

$$B_{45} = - B_{36}, \qquad \text{(42 cont.)}$$

$$B_{46} = B_{35}$$

and

$$B_{53} = B_{64} = 1,$$

where c and k are damping and stiffness coefficients which appear in the internal torque.

The term $\underline{T}$ in Eq. (41) is due to the mechanical thrust misalignment and has the form

$$\underline{T} = [-\alpha_y F_T \ell_c - \alpha_z F_T \ell_c \quad 0 \quad 0 \quad 0 \quad 0]^T , \qquad (43)$$

where $\ell_c = [\ell_1 m_1 + (\ell_1 + r_1 + r_2)m_2]/M$.

The complete set of linearized, rotational motion equations consists of Eqs. (35a), (35b), (36), (40) and (41). These equations, although linear, have variable coefficients if $\Omega_1$ is not constant. In the next section, the additional assumption that $\Omega_1$ is constant is made and closed-form solutions for $\Omega_2$, $\Omega_3$, $\omega_2$, $\omega_3$, $\theta_2$, $\theta_3$, $\Theta$ and $\Psi$ are obtained.

## 2.4 Solution to the Linear Equations when Spin Rate is Constant and Nonzero

When spin rate, $\dot{\phi} = \Omega_1$, is constant, the matrix $\underline{B}$ of Eq. (41) is constant. In this case, the linear equations are time invariant and may be solved exactly by elementary methods. Once the solution for $\underline{x}(t)$ is obtained, the elements $x_1 = \Omega_2$ and $x_2 = \Omega_3$ may be inserted into Eqs. (35a) and (35b) and solutions for $\Psi$ and $\Theta$ obtained by directly integrating with respect to time.

We first consider the homogeneous equation $\underline{\underline{I}}\dot{\underline{x}} = \underline{\underline{B}}\underline{x}$ and let

$$\underline{\underline{A}} = \underline{\underline{I}}^{-1}\,\underline{\underline{B}} \ ,$$

when $\Omega_1$ is constant. Hence, the system of equations to be solved is

$$\dot{\underline{x}} = \underline{\underline{A}}\,\underline{x} \ , \tag{44}$$

where $\underline{\underline{A}}$ is a constant 6x6 matrix. It is well known that the general solution to Eq. (44) is composed of six linearly independent solutions of the form,

$$\underline{y}_j = \underline{e}_j\, e^{\lambda_j t} \ , \tag{45}$$

where $\underline{e}_j$ is an eigenvector of $\underline{\underline{A}}$ and $\lambda_j$ is the corresponding eigenvalue. The eigenvalues are zeros of the function,

$$f(\lambda) = |\lambda\underline{\underline{I}} - \underline{\underline{A}}| \ , \tag{46}$$

where $\underline{\underline{I}}$ is the 6x6 identity matrix and $|\ \ |$ denotes the determinant. The eigenvectors $\underline{e}_j$ are such that

$$\underline{\underline{B}}(\lambda_j)\underline{e}_j = \underline{0} \qquad (j=1,2,3,\ldots,6) \ , \tag{47}$$

where $\underline{\underline{B}}(\lambda_j) = \lambda_j\,\underline{\underline{I}} - \underline{\underline{A}}$ .

For the particular problem of interest, when $\Omega_1 \neq 0$, the eigenvalues and eigenvectors generally occur in complex conjugate pairs. From this fact we conclude that the homogeneous solution for each element of $\underline{x}$ is the superposition of six trigonometric terms, each of which is multiplied by an exponential function of time.

We define $\underline{\underline{E}}$ to be a 6x6 matrix, the odd columns of which are composed the real parts of eigenvectors corresponding to three eigenvalues, none of which are complex conjugates of another and each of which has a positive imaginary part.

The even columns of $\underline{\underline{E}}$ are composed of the negatives of the imaginary parts of the chosen eigenvectors. We also let $n_j$ denote the real part of $\lambda_j$, and $\omega_j$ (not to be confused with $\omega_2$ or $\omega_3$ of the previous subsections) the imaginary part of $\lambda_j$. The homogeneous solution for $\underline{x}$ may then be written as

$$\underline{x}_h(t) = \underline{\underline{E}}^{-1}\,\underline{\underline{D}}\,\underline{\underline{E}}\,\underline{x}_o \ , \tag{48}$$

where $\underline{x}_o = x(t_o)$ and, with $\tau = t - t_o$,

$$\underline{\underline{D}} = \begin{bmatrix} \underline{\underline{D}}_{11} & \underline{\underline{0}} & \underline{\underline{0}} \\ \underline{\underline{0}} & \underline{\underline{D}}_{22} & \underline{\underline{0}} \\ \underline{\underline{0}} & \underline{\underline{0}} & \underline{\underline{D}}_{33} \end{bmatrix} . \tag{49}$$

In Eq. (49),

$$\underline{\underline{D}}_{jj} = \begin{bmatrix} e^{n_j\tau}\cos\omega_j\tau & e^{n_j\tau}\sin\omega_j\tau \\ -e^{n_j\tau}\sin\omega_j\tau & e^{n_j\tau}\cos\omega_j\tau \end{bmatrix} \quad (j=1,2,3) \ . \tag{50}$$

Equation (48) can also be written as

$$\underline{x}_h(t) = \underline{\underline{\Phi}}(t,t_o)\underline{x}_o \ ,$$

where $\underline{\underline{\Phi}}$ is the state transition matrix.

Solution for $\Psi$ and $\Theta$

To integrate Eqs. (35a) and (35b), we need to replace $\Omega_2$ and $\Omega_3$ by their explicit solutions, $\Phi$ by $\Omega_1\tau$ and integrate each equation term by term. Dropping the subscript h for the present, we write the solutions for the $x_j$ in the explicit forms,

$$x_j = \sum_{i=1}^{3} e^{n_i\tau}(A_{ij}\cos\omega_i\tau + B_{ij}\sin\omega_i\tau) \quad (j=1,2,..,6) \ , \tag{51}$$

where, if $E_{jk}$ is an element of $\underline{\underline{E}}$ and $C_j$ is an element of $\underline{C} = \underline{\underline{E}}^{-1}\,\underline{x}_o$ ,

$$A_{ij} = E_{j,2i-i}\,C_{2i-1} + E_{j,2i}\,C_{2i} \tag{52a}$$

and

$$B_{ij} = E_{j,2i-1}\,C_{2i} - E_{j,2i}\,C_{2i-1}\,. \tag{52b}$$

Since $\Omega_2 \equiv x_1$ and $\Omega_3 \equiv x_2$, the desired expressions for these variables are available and, upon inserting them into Eqs. (35a) and (35b), we obtain (assuming $\Phi_o \triangleq \Phi(t_o) = 0$)

$$\begin{aligned}\dot{\Theta} = \frac{1}{2}\sum_{i=1}^{3} e^{n_i\tau}\{&(A_{i1}-B_{i2})\cos p_i\tau \\ &+ (A_{i1}+B_{i2})\cos q_i\tau \\ &- (A_{i2}+B_{i1})\sin p_i\tau \\ &- (A_{i2}-B_{i1})\sin q_i\tau\}\end{aligned} \tag{53a}$$

and

$$\begin{aligned}\dot{\Psi} = \frac{1}{2}\sum_{i=1}^{3} e^{n_i\tau}\{&(A_{i2}+B_{i1})\cos p_i + (A_{i2}-B_{i1})\cos q_i\tau \\ &+ (A_{i1}-B_{i2})\sin p_i\tau + (A_{i1}+B_{i2})\sin q_i\tau\},\end{aligned} \tag{53b}$$

where $p_i = \Omega_1 - \omega_i$ and $q_i = \Omega_1 + \omega_i$. Equations (53) may also be written in the matrix form,

$$\begin{bmatrix}\dot{\Theta}\\ \dot{\Psi}\end{bmatrix} = \frac{1}{2}\sum_{i=1}^{3}\begin{bmatrix}\cos p_i\tau & -\sin p_i\tau\\ \sin p_i\tau & \cos p_i\tau\end{bmatrix}\begin{bmatrix}A_{i1}-B_{i2}\\ A_{i2}+B_{i1}\end{bmatrix} e^{n_i\tau}$$

$$+\frac{1}{2}\sum_{i=1}^{3}\begin{bmatrix}\cos q_i\tau & -\sin q_i\tau\\ \sin q_i\tau & \cos q_i\tau\end{bmatrix}\begin{bmatrix}A_{i1}+B_{i2}\\ A_{i2}-B_{i1}\end{bmatrix} e^{n_i\tau}, \qquad (54)$$

from which the orthogonality of $\dot{\Theta}$ and $\dot{\Psi}$ may be seen.

The integration of Eq. (54) is straightforward and the result we obtain is

$$\begin{bmatrix}\Theta\\ \Psi\end{bmatrix} = \frac{1}{2}\sum_{i=1}^{3}\frac{e^{n_i\tau}}{n_i^2+p_i^2}\,\underline{P}(\tau)\begin{bmatrix}A_{i1}-B_{i2}\\ A_{i2}+B_{i1}\end{bmatrix}$$

$$+\frac{1}{2}\sum_{i-1}^{3}\frac{e^{n_i\tau}}{n_i^2+q_i^2}\,\underline{Q}(\tau)\begin{bmatrix}A_{i1}+B_{i2}\\ A_{i2}-B_{i1}\end{bmatrix}, \qquad (55)$$

where

$$\underline{P}(\tau)=\begin{bmatrix}n_i(cp_i\tau-1)+p_i sp_i\tau & -[n_i sp_i\tau-p_i(cp_i\tau-1)]\\ n_i[sp_i\tau-p_i(cp_i\tau-1)] & n_i(cp_i\tau-1)+p_i sp_i\tau\end{bmatrix} \qquad (56)$$

and $\underline{Q}(\tau)$ has the same form as $\underline{P}(\tau)$, but in $\underline{Q}(\tau)$ the $q_i$ take the place of the $p_i$.

Equations (51) and (55) along with $\Phi = \Omega_1\tau$ constitute the complete solution for the rotation motion of the two parts of the rocket model when there is no mechanical thrust misalignment. To use the solutions it is only necessary to (1) determine the eigenvalues and eigenvectors of the matrix $\underline{A}$, (2) form $\underline{E}$,

(3) invert $\underline{\underline{E}}$, (4) form $\underline{c} = \underline{\underline{E}}^{-1}\,\underline{x}_o$, (5) determine $A_{ij}$ and $B_{ij}$, (6) determine $p_i$ and $q_i$, (7) substitute the time at which the solution is to be evaluated into the equations, and (8) calculate the values of the variables.

Thrust Misalignment Effects

Because the solution to the linearized equations for the case when the thrust vector is not aligned with the $x_1$-axis will be needed in the next subsection, we consider here the problem of obtaining such a solution. This requires that we find the general solution to the nonhomogeneous equation (41), or equivalently, the equation,

$$\dot{\underline{x}} = \underline{\underline{A}}\underline{x} + \underline{f} \ , \tag{57}$$

where

$$\underline{f} = \underline{\underline{I}}^{-1}[-\alpha_y F_T \ell_c \, , -\alpha_z F_T \ell_c \, , 0 \, , 0 \, , 0 \, , 0]^T . \tag{58}$$

The solution for $\underline{x}(t)$ in this case is composed of the solution to $\dot{\underline{x}} = \underline{\underline{A}}\underline{x}$, i.e., the homogeneous solution $\underline{x}_h$, plus a particular solution. Since $\underline{f}$ is constant, a particular solution is

$$\underline{x}_p = - \underline{\underline{A}}^{-1}\underline{f} \ . \tag{59}$$

The solution $\underline{x} = \underline{x}_h + \underline{x}_p$ is subject to the initial conditions $\underline{x}_o = \underline{x}(0)$. Thus, $\underline{x}_h(0) = \underline{x}_o - \underline{x}_p$ and the constants which appear in the homogeneous part of the solution are determined from Eq. (48) with $\underline{x}_h(0)$ in place of $\underline{x}_o$.

When thrust misalignment effects are present, the solutions for $\Omega_2 \equiv x_1$ and $\Omega_3 \equiv x_2$ have the extra terms $x_{1p}$ and $x_{2p}$ and those for $\Theta$ and $\Psi$ have the additional terms $(x_{1p}/\Omega_1)\sin\Phi + (x_{2p}/\Omega_1)(\cos\Phi - 1)$ and $(x_{1p}/\Omega_1)(1-\cos\Phi) + (x_{2p}/\Omega_1)\sin\Phi$, respectively. The effects of these terms will be discussed in the next subsection,

but, generally speaking, their inclusion results in periodic variations in $\Theta$ and $\Psi$ at the spin frequency. Furthermore, the inclusion of the effects of thrust misalignment in this form (i.e., constant thrust) results in changes in the bending amplitudes and rates because $\underline{x}_h(0)$ and not $\underline{x}_o$ is used to obtain these.

For all cases considered to date, one of the complex pairs of eigenvalues has a very small magnitude real part and an imaginary part very nearly equal to the spin frequency. Numerically, this small magnitude real part is sometimes negative. The other two are always negative if damping is present. That the small magnitude real part was sometimes found to be positive was at first surprising, because it implies that the motion is asymptotically stable, although the spin is nominally about the axis of minimum moment of inertia. At first sight, this result appears inconsistent with the popular "maximum moment of inertia spin criterion" of spacecraft attitude dynamics, which states that torque-free spin of a quasi-rigid† body about its axis of moment of inertia is unstable when there is inertial dissipation.[11] The key difference in the spacecraft case and the two-body rocket is that the spacecraft must be quasi-rigid for the criterion to apply to the two-body rocket is not quasi rigid, since the parts which move relative to each other are of essentially equal mass. To verify that this is, in fact, a reason for the different results, the second body of the two-body rocket model was replaced by a small point mass attached to a massless rigid rod hinged to Body 1 at point R. The eigenvalues for this "spacecraft" model were calculated and one of the three complex conjugate pairs possesses a positive real part. Hence, it appears that the relative size of the two bodies and/or lack of sufficient numerical precision causes this anomaly.

†The moving parts of the spacecraft have small mass compared to the total spacecraft mass.

Actually, for our purposes, it is not very important if the small magnitude real part is positive, or negative, as long as its magnitude is small compared to those of the other real parts and small compared to the reciprocal of the time period of interest. For, if this is the case, the other two modes will rapidly die out leaving the lightly damped mode as the dominant motion.

The lightly damped mode is of special interest because, generally, it is essentially a "rigid-body" mode in which very little relative motion between the two parts of the rocket exists. If the two parts of the rocket are identical, it is exactly a rigid-body mode. Furthermore, the frequency of the lightly damped mode is essentially the rigid-body nutation frequency so that when $\dot{\Theta}$ and $\dot{\Psi}$ are formed their parts due to their mode are long-period, lightly-damped oscillations. In a plot covering a time period much smaller than the long-period of these oscillations, they appear as straight lines. Hence, we are led to define a "steady-state transverse rate" $\dot{\theta}_{ss}$ as the square root of the sum of the squares of the coefficients of the sine and cosine terms of lightly damped parts of $\Omega_2 = x_1$. The square root of the sum of the squares of the corresponding coefficients in the $\Omega_3 = x_2$ solution is the same, i.e., $\Omega_2$ and $\Omega_3$ are orthogonal.

The quantity $\dot{\theta}_{ss}$ is felt to be a good measure of the adverse transverse rate caused by bending and thrust misalignment, the effects of which are incorporated in it through $\underline{x}_h(0) = \underline{x}_o - \underline{x}_p$.

## 2.5 Results from the Solution to the Linear Equations

Although the solution given in subsection 2.4 is in closed form, it is not explicit enough that the effects of changes of system parameters can be

determined without numerical computations. Hence, a digital computer code (FORTRAN IV) for evaluating the solution was developed. It is completely "self-contained" in that no system subroutines are needed (except for plotting). For the most part, it is a linear system analysis code which takes given values of the system constants and (1) generates the matrices $\underline{\underline{I}}$, $\underline{\underline{B}}$ and $\underline{T}$, (2) forms $\underline{\underline{A}} = \underline{\underline{I}}^{-1}\underline{\underline{B}}$ and $\underline{f} = \underline{\underline{A}}^{-1}\,\underline{T}$, (3) determines the eigenvalues and eigenvectors of $\underline{\underline{A}}$, and (4) prints out the explicit numerical form of the solution for $\underline{x}(t)$ and those for $\Theta(t)$, $\Psi(t)$, $\Theta_N(t)$ and $\Psi_N(t)$ at various time points and (6) stores these values for plotting. A working version of this code has been made available to U.S. Army personnel.

The code was used to obtain the results presented in this subsection. These results include "general" parametric results and some results for a specific rocket model which are compared with test data. The "general" parametric results were obtained by adopting a baseline rocket model, determining its nominal behavior and then varying one of the system parameters. The characteristics of the baseline, or nominal (N), rocket model are given in Table 1. The rocket model's two parts were assumed to be homogeneous, right circular cylinders of equal radius and their moments of inertia were computed from standard formulas. This method of computing the moments of inertia results values for the overall moments of inertias which are approximately the same as those of an actual free-flight rocket . The length $\ell_1+r_1$ was chosen so that the center of mass of the rocket model is at the hinge point. This was done so the first bending mode should be well approximated when the two bodies are identical. It is <u>not</u> a <u>necessary</u> requirement.

Table 1. Physical characteristics of the baseline model.

| Body 1 | | Body 2 | |
|---|---|---|---|
| $m_1$ | 50.466 kg | $m_2$ | 64.286 kg |
| $\ell_1$ | 0.938 m | $\ell_2$ | -0.335 m |
| $r_1$ | 0.938 m | $r_2$ | 0.739 m |
| Radius | 0.095 m | Radius | 0.095 m |
| $A_1$ | 0.228 kg-m$^2$ | $B_1$ | 0.290 kg-m$^2$ |
| $A_2$ | 14.91 kg-m$^2$ | $B_2$ | 11.86 kg-m$^2$ |

| | |
|---|---|
| $F_T$ | 44482 Nt |
| $I_T$ | 106.29 kg-m$^2$ |
| $I_x$ | 0.518 kg-m$^2$ |

The initial conditions used to obtain all the results given in this subsection were determined by specifying the initial transverse angular deflections and rates of the nose of the rocket and requiring that the line segment PQ be nonrotating initially as it would be in a launch from an ideally rigid launcher. Also, a zero initial roll angle is assumed. These conditions are sufficient to obtain the initial conditions $x_{j0}$. Explicitly,

$$
\begin{aligned}
x_{10} &= -[(\ell_2 + r_2)/(\ell_1 + r_1)][\Psi_{NO}\Omega_1 + \dot{\Theta}_{NO}) \ , \\
x_{20} &= -[(\ell_2 + r_2)/(\ell_1 + r_1)](-\Theta_{NO}\Omega_1 + \dot{\Psi}_{NO}) \ , \\
x_{30} &= -[(d/(\ell_2 + r_2)]\ x_{10} \ , \\
x_{40} &= -[(d/(\ell_2 + r_2)]\ x_{20} \ , \\
x_{50} &= [d/(\ell_1 + r_1)]\ \Theta_{NO} \ , \\
x_{60} &= [d/(\ell_1 + r_1)]\ \Psi_{NO} \ , \\
\Psi_o &= -[(\ell_2 + r_2)/d]\ x_{50}
\end{aligned}
\qquad (60)
$$

and

$$
\Theta_o = -[(\ell_2 + r_2)/d]\ x_{60} \ ,
$$

where $d = \ell_1 + r_1 + \ell_2 + r_2$.

The initial conditions for the nominal case were obtained using the above equations and $\Psi_{NO} = 0.0001$ rad., $\Theta_{NO} = \dot{\Psi}_{NO} = \dot{\Theta}_{NO} = 0$. The time history of $\Psi_N$ is shown in Fig. 6. The mean value of $\Psi_N$ is very slightly decreasing and the damping is apparent in that the amplitude of the bending oscillations is noticeably decreasing with time. The primary effect of non-zero $\Psi_N$ initially is seen in the plot of $\Theta_N$ as a function of time in Fig. 7. It is a secular change in $\Theta_N$ of $-1.213 \times 10^{-3}$ rad/sec. There are no bending oscillations apparent in the $\Theta_N$ curve until the Coriolis coupling terms transfer some of the bending present in $\Psi_N$ into the pitch plane.

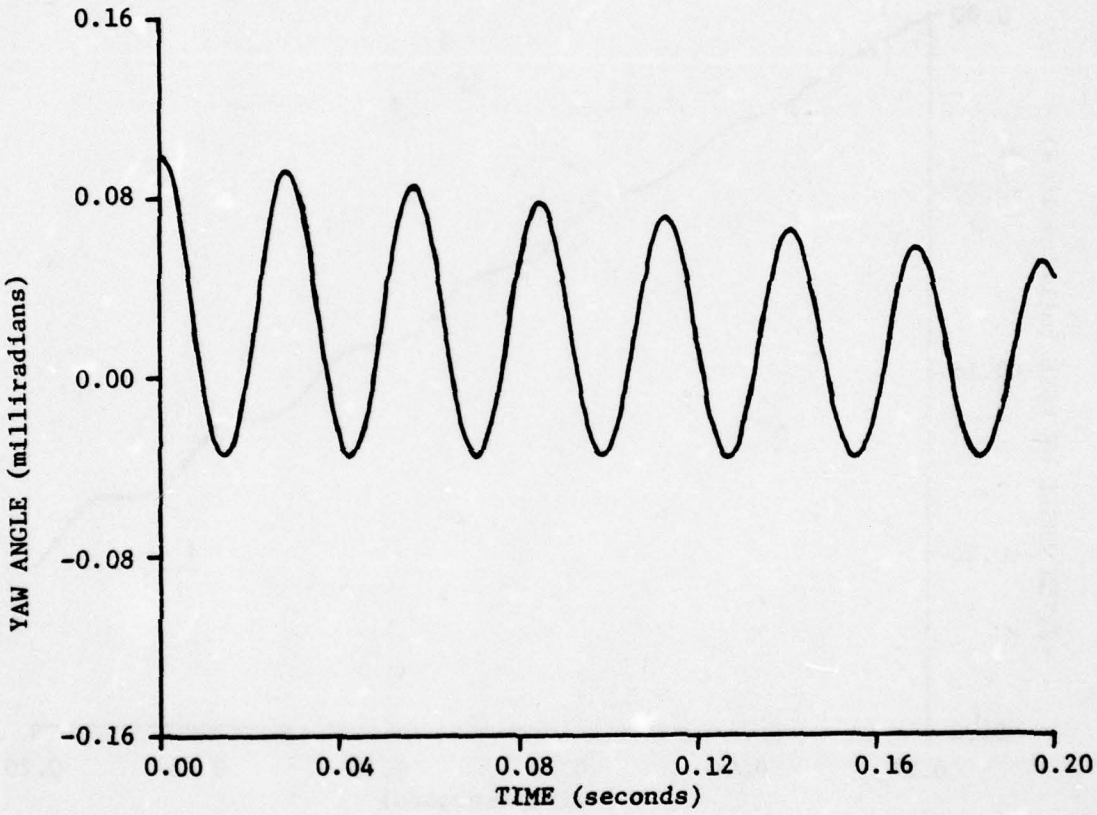


**Figure 6. Time history of yaw angle of rocket's nose.**

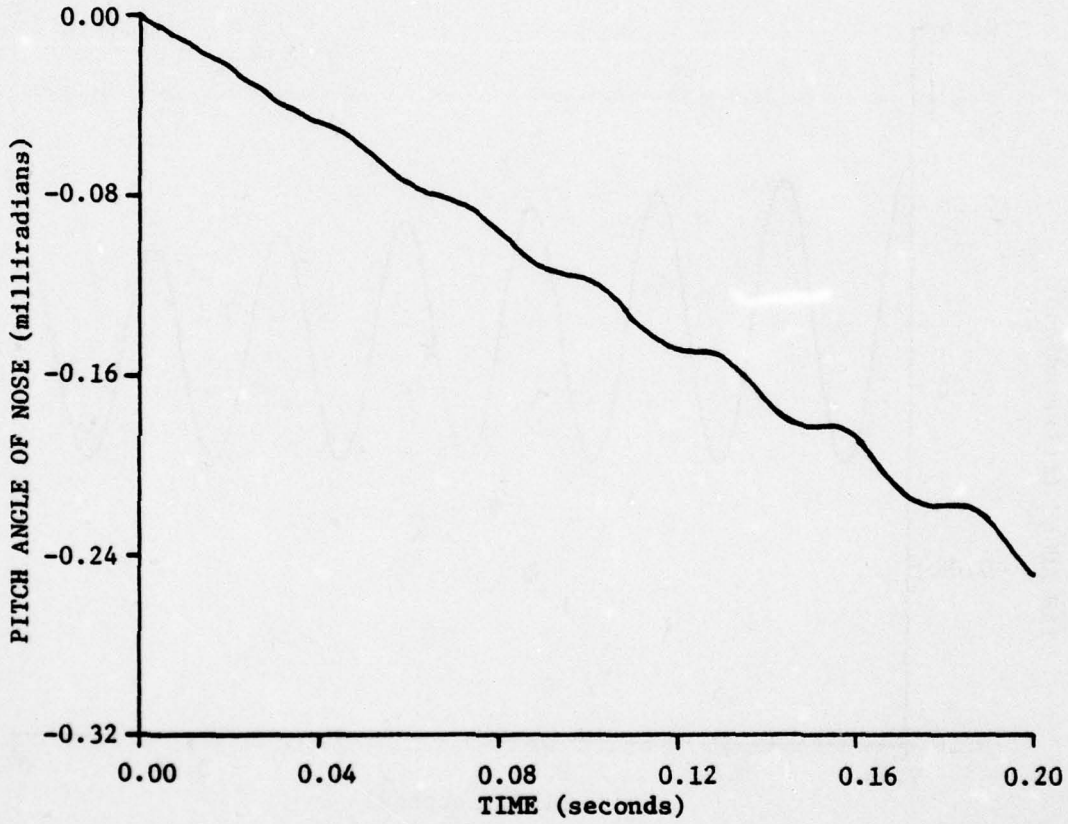


Figure 7. Time history of pitch angle of rocket's nose.

Because the spin rate influences the "steady-state" rate greatly, values of $\dot{\Theta}_{ss}$ were determined for various spin rates in addition to those listed in Table 2. For the case of only bending of magnitude 0.0001 radians, the results are shown in Fig. 8. The variation of $\dot{\Theta}_{ss}$ as a function of spin rate is linear. When "additive" mechanical thrust misalignment (Case 1) is also present, the variation of $\dot{\Theta}_{ss}$ with spin rate has a minimum at about 9 Hz (see Fig. 9).

A Specific Example

Optical lever data are available for several rockets flight tested during an experimental program.[12] Some of these rockets apparently bent transversely a good deal if the data is assumed to be accurate to say ±0.0001 rad. Hence, it was decided to test the adequacy of the two-body rocket model by trying to match the optical lever data of one rocket with $\Theta_N$ and $\Psi_N$ time histories generated using the solution.

The rocket chosen to be modeled was the GEM #7. That rocket was spun up using an eroding spin turbine, so its spin rate was not constant. A mean rate of 47 rad/sec was therefore chosen because the two-body solution requires a constant spin rate. The other characteristics of GEM #7 are given in Table 3.

The optical lever data obtained during the flight of GEM #7 were used to determine the "mean" rates of the yaw and pitch angles of that rocket's nose. These were taken as -0.0097 and 0.036 rad/sec, respectively. Also, from the data, the values of $\Psi_N$, $\Theta_N$, $\dot{\Psi}_N$ and $\dot{\Theta}_N$ due to bending at the end of guidance were estimated. These values are as follows:

$\Psi_{NO}$ = 0.00025 radians, $\Theta_{NO}$ = -0.00025 radians, $\dot{\Psi}_{NO}$ = 0.0 rad/sec and $\dot{\Theta}_{NO}$ = 0.364 rad/sec.

Table 2. Parametric results with initial bending in yaw plane.

| Parameter \ Case | N | 1 | 2 | 3 | 4 | 5 | 6 | 7 | 8 | 9 | 10 |
|---|---|---|---|---|---|---|---|---|---|---|---|
| $\alpha_z$ (rad) | 0 | -0.0001 | 0.0001 | N | N | N | N | N | N | N | N |
| $\Omega_1$ (Hz) | 9 | N | N | 3 | 15 | N | N | N | N | N | N |
| $\ell_2$ (m) | -0.3354 | N | N | N | N | 0 | 0.3354 | N | N | N | N |
| k (Nt-m) | $3.39 \times 10^5$ | N | N | N | N | N | N | $1.356 \times 10^6$ | $8.473 \times 10^5$ | N | N |
| c (Nt-m/sec) | 27.12 | N | N | N | N | N | N | N | N | 0.271 | 2712 |
| $\dot{\theta}_{ss}$ (mrad/sec) | 1.213 | 2.574 | 0.147 | 0.405 | 1.618 | 2.224 | 3.234 | 1.214 | 1.213 | 1.213 | 1.288 |

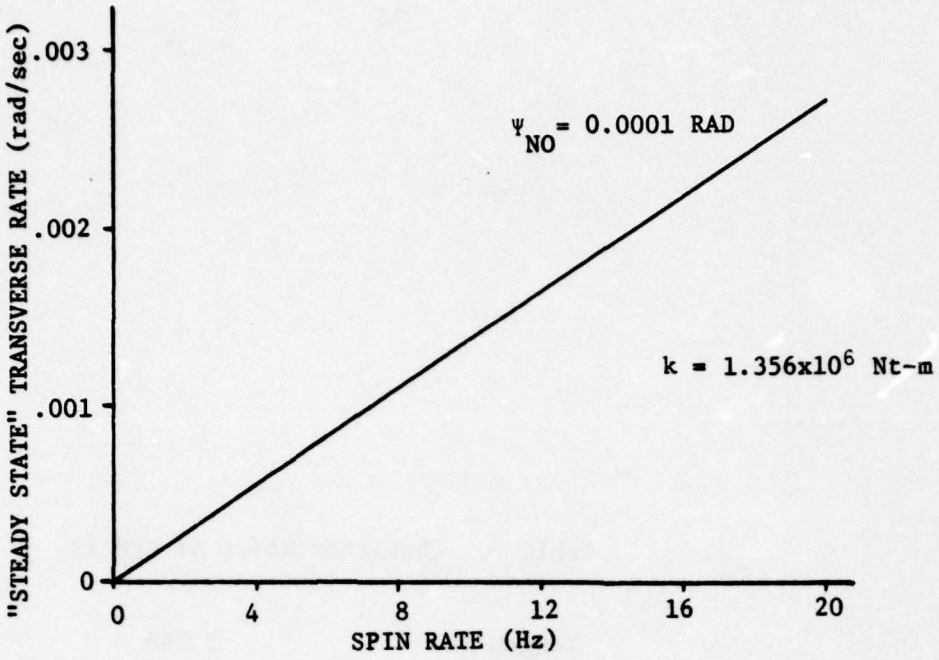


Figure 8. Effect of spin rate on "steady-state" rate due to bending.

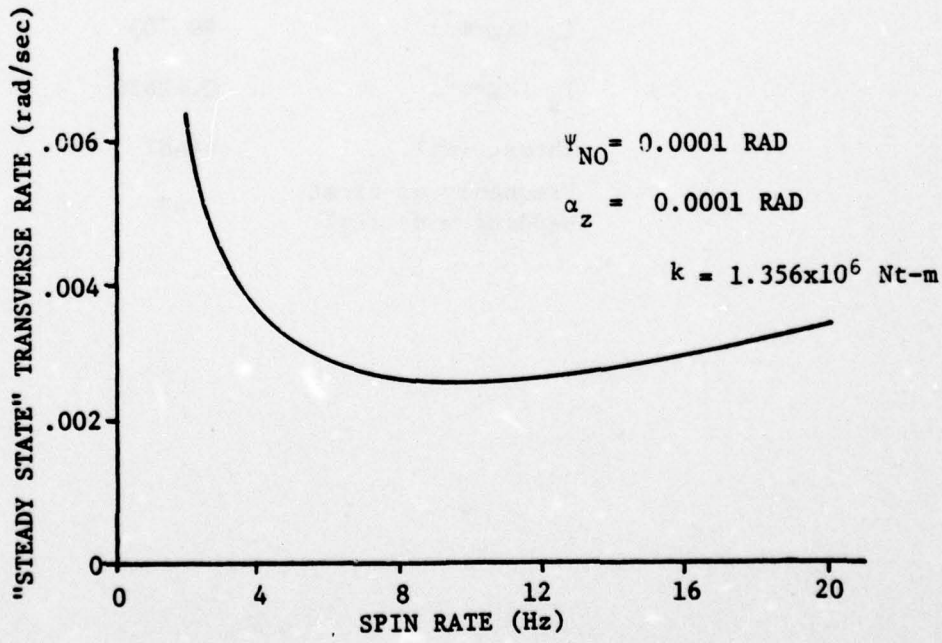


Figure 9. Effect of spin rate on "steady-state" rate due to bending and mechanical thrust misalignment.

Table 3. Characteristics of GEM #7

| | |
|---|---|
| Length (m) | 3.348 |
| Radius at aft end (m) | 0.1575 |
| Mass (kg) | 114.76 |
| $I_T$ (kg-$m^2$) | 99.705 |
| $I_x$ (kg-$m^2$) | 0.40636 |
| Thrust (Nt) | 44482 |
| Frequency of first bending mode (Hz) | 67 |

The model characteristics given in Table 4 were developed from the actual characteristics of the rocket. Note that $I_T$ and $I_x$ for the model are not exactly those of the actual rocket because of the use of right circular cylinders to model the two parts of the rocket.

The three frequencies of the two-body model are 82.8 Hz, 68 Hz, and 7.44 Hz. The characteristics of the solution are such that the "bending" frequency of the model is 68 Hz and the lowest frequency is the model's nutation frequency.

To determine the amount of thrust misalignment (an equivalent amount of mass imbalance could be substituted) which results in the mean rate cited above, the two-body computer code was run six times with $\Psi_{NO}$, $\Theta_{NO}$, $\dot{\Psi}_{NO}$, $\dot{\Theta}_{NO}$, $\alpha_y$ and $\alpha_z$ successively equal numerically to 0.001. From the six runs, "sensitivity" coefficients were determined. These, when multiplied by the given values of the initial values of yaw and pitch angles and their time rates of change, and the appropriate thrust misalignment angles, result in the desired mean rates. The values of $\alpha_y$ and $\alpha_z$ thus obtained are 0.0006765 and -0.004598 radians, respectively. These values are within the realm of physical possibility.

By running the two-body model computer program with the values given above, plots of $\Theta_N$ and $\Psi_N$ versus time were generated. These plots were time-shifted to match the phase of the experimental data. A shifting was also made to eliminate the bias of the data. The resulting theoretical time histories are shown as the solid curves in Fig. 10. The dashed curves were obtained from Ref. 12 and represent smoothed optical lever data. The time 0.15 seconds on the plots corresponds to the end of guidance time of

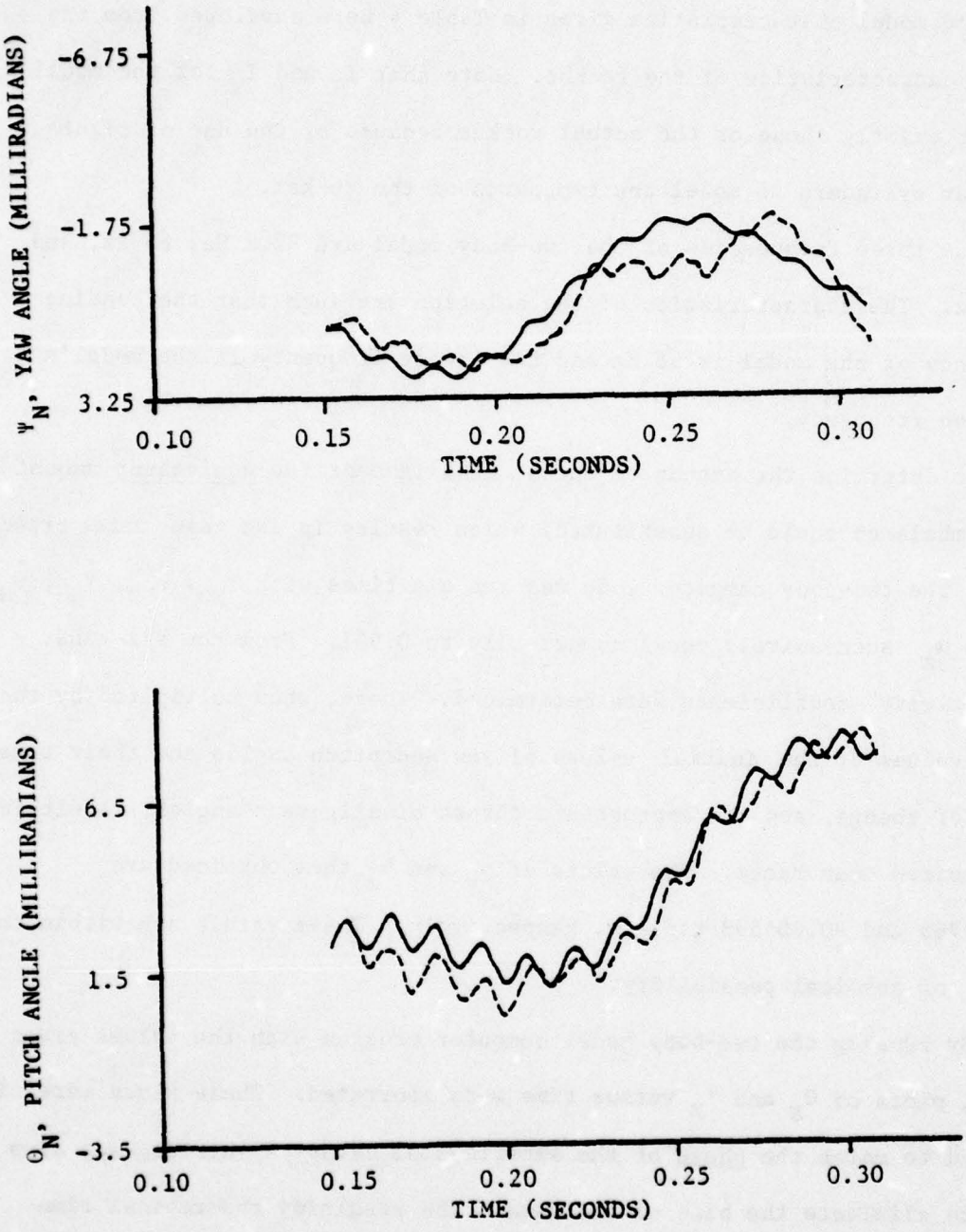


Figure 10. Comparison of flight test data and theoretical results.

0.1901 seconds. Very good agreement is apparent, although the model is a simple one. In particular, only the first bending mode is modeled and, since a constant spin rate is used in generating the analytical solution, the variable spin rate of the actual rocket is not precisely modeled. We conclude that the simple two-body model can be used to analyze optical lever data which contains evidence of rocket transverse bending.

An important observation which may be made concerning these results is that, on the basis of the model, the bending of the rocket contributed a transverse rigid body rate at launch of magnitude 0.115 rad/sec. The thrust misalignment was, in this particular case, such that it opposed the effect of bending so that the observed transverse rate at launch was less than that due solely to bending.

Table 4. Characteristics of two-body model of GEM #7

| Body 1 | | Body 2 | |
|---|---|---|---|
| $m_1$ (kg) | 50.466 | $m_2$ (kg) | 64.286 |
| $\ell_1$ (m) | 0.9376 | $\ell_2$ (m) | -0.3354 |
| $r_1$ (m) | 0.9376 | $r_2$ (m) | 0.7393 |
| Radius (m) | 0.095 | Radius (m) | 0.095 |
| $A_1$ (kg-m$^2$) | 0.2279 | $B_1$ (kg-m$^2$) | 0.2903 |
| $A_2$ (kg-m$^2$) | 14.909 | $B_2$ (kg-m$^2$) | 11.857 |
| | | k (Nt-m) | $1.491 \times 10^6$ |
| | | $F_T$ (Nt) | 44482 |
| | | $I_T$ (kg-m$^2$) | 106.29 |
| | | $I_x$ (kg-m$^2$) | 0.5182 |

## 2.6 Nonlinear Equations for Motion on a Rigid Launcher

As stated in Section 1, the equations for motion on a rigid launcher were not developed until near the end of this study. Because of this, they were not used to obtain initial conditions for the free-flight phase equations given supra. This is not considered to detract from the results given in the preceding section, however, because the initial conditions used to obtain those results are representative of those measured during flight tests.

The launch-phase equations are given here for the purposes of (1) "completing" the model and (2) providing a means of studying the motion of a two-body rocket ideally constrained on a rigid launcher. An obvious, and probably needed, extension of the equations given in this subsection would be to include a launcher model with three or more degrees of freedom.

### Constraints

While on the launcher, the points P and Q are constrained to travel along the $x_L$-axis of the launcher coordinate frame $Ox_Ly_Lz_L$ shown in Fig. 11. The two bodies therefore have four degrees of freedom during the launch phase. These may be chosen to be:(1) the displacement of the point P along the $x_L$-axis, $x_p$; (2) the yaw angle of Body 1 relative to the $x_L$-axis, $\Psi$; (3) the pitch angle of Body 1 relative to the $Ox_Ly_Lz_L$ frame, $\theta$; (4) the roll angle of Body 1 about the $x_1$-axis.

The orientations of the unit vector triads ($\hat{\underline{i}}_L$, $\hat{\underline{j}}_L$, $\hat{\underline{k}}_L$), ($\hat{\underline{i}}_1$, $\hat{\underline{j}}_1$, $\hat{\underline{k}}_1$) and ($\hat{\underline{i}}_2$, $\hat{\underline{j}}_2$, $\hat{\underline{k}}_2$) relative to each other and to the inertial reference frame unit vector triad ($\hat{\underline{I}}$, $\hat{\underline{J}}$, $\hat{\underline{K}}$) are defined by the following equations:

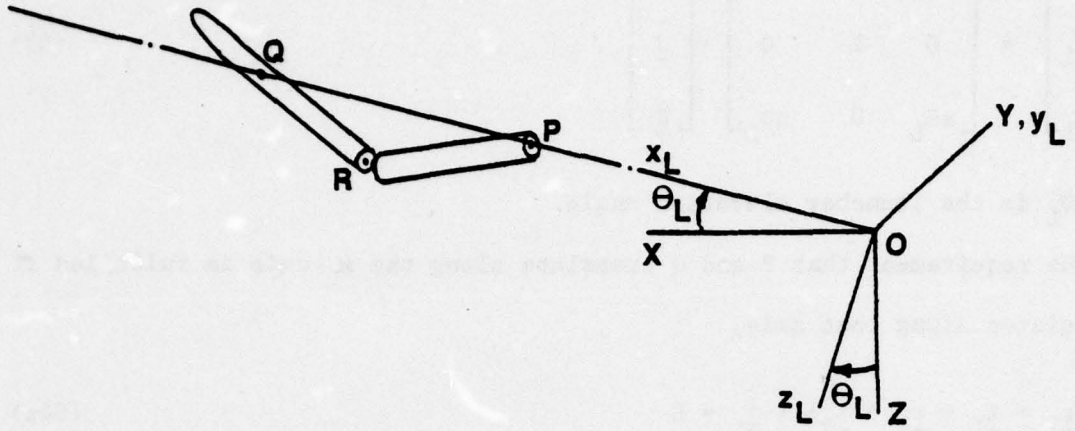


Figure 11. Two-body rocket model geometry during launch phase.

$$\begin{bmatrix} \hat{\underline{i}}_2 \\ \hat{\underline{j}}_2 \\ \hat{\underline{k}}_2 \end{bmatrix} = \underline{\underline{A}} \begin{bmatrix} \hat{\underline{i}}_1 \\ \hat{\underline{j}}_1 \\ \hat{\underline{k}}_1 \end{bmatrix} , \tag{61}$$

$$\begin{bmatrix} \hat{\underline{i}}_1 \\ \hat{\underline{j}}_1 \\ \hat{\underline{k}}_1 \end{bmatrix} = \underline{\underline{B}} \begin{bmatrix} \hat{\underline{i}}_L \\ \hat{\underline{j}}_L \\ \hat{\underline{k}}_L \end{bmatrix} , \tag{62a}$$

$$\underline{\underline{B}} = \begin{bmatrix} 1 & 0 & 0 \\ 0 & c\phi & s\phi \\ 0 & -s\phi & c\phi \end{bmatrix} \begin{bmatrix} c\theta & 0 & -s\theta \\ 0 & 1 & 0 \\ s\theta & 0 & c\theta \end{bmatrix} \begin{bmatrix} c\psi & s\psi & 0 \\ -s\psi & c\psi & 0 \\ 0 & 0 & 1 \end{bmatrix} , \tag{62b}$$

$$\begin{bmatrix} \hat{\underline{i}}_L \\ \hat{\underline{j}}_L \\ \hat{\underline{k}}_L \end{bmatrix} = \begin{bmatrix} c\Theta_L & 0 & -s\Theta_L \\ 0 & 1 & 0 \\ s\Theta_L & 0 & c\Theta_L \end{bmatrix} \begin{bmatrix} \hat{\underline{I}} \\ \hat{\underline{J}} \\ \hat{\underline{K}} \end{bmatrix}, \tag{63}$$

where $\Theta_L$ is the launcher elevation angle.

The requirement that P and Q translate along the $x_L$-axis is fulfilled if P translates along that axis,

$$(\underline{r}_1 + \underline{\ell}_1 + \underline{r}_1 + \underline{\ell}_2) \cdot \hat{\underline{j}}_L = 0 \tag{64a}$$

and

$$(\underline{r}_1 + \underline{\ell}_1 + \underline{r}_2 + \underline{\ell}_2) \cdot \hat{\underline{k}}_L = 0 \, . \tag{64b}$$

Now, assuming that $\underline{r}_1 = (r_1 \quad 0 \quad 0)^T$, $\underline{\ell}_1 = (\ell_1 \quad 0 \quad 0)^T$, $\underline{r}_2 = (r_2 \quad 0 \quad 0)^T$ and $\underline{\ell}_2 = (\ell_2 \quad 0 \quad 0)^T$ and that $\theta_2$, $\theta_3$, $\psi$ and $\theta$ are small angles (which certainly should be the case), Eqs. (61), (62) and (64) can be used to obtain the following result:

$$\begin{bmatrix} \theta_2 \\ \theta_3 \end{bmatrix} = - R \begin{bmatrix} c\phi & s\phi \\ -s\phi & c\phi \end{bmatrix} \begin{bmatrix} \theta \\ \psi \end{bmatrix}, \tag{65}$$

where $R = (r_1 + \ell_1 + r_2 + \ell_2)/(r_2 + \ell_2)$.[†] By differentiating Eq. (65) with respect to time and using the approximate equations,

$$\Omega_1 = \dot{\phi} \, , \tag{66a}$$

$$\Omega_2 = \dot{\theta} c\phi + \dot{\psi} s\phi \tag{66b}$$

and

$$\Omega_3 = -\dot{\theta} s\phi + \dot{\psi} c\phi, \tag{66c}$$

[†]If $\ell_2 < 0$, then $r_2$ must not be equal to $|\ell_2|$.

we obtain

$$\begin{bmatrix} \dot{\theta}_2 \\ \dot{\theta}_3 \end{bmatrix} = \Omega_1 \begin{bmatrix} \theta_3 \\ -\theta_2 \end{bmatrix} - R \begin{bmatrix} \Omega_2 \\ \Omega_3 \end{bmatrix} . \tag{67}$$

The <u>total</u> angular velocity of Body 2 in the Body 2 basis is denoted $\underline{\omega}_2$. Since $\underline{\omega}_2 = \underline{\underline{A}}\ \underline{\Omega}_1 + \underline{\omega}_{2/1}$ and $\underline{\omega}_{2/1} \simeq (0 \quad \dot{\theta}_2 \quad \dot{\theta}_3)^T$, we find that

$$\underline{\omega}_2 \simeq (\Omega_1 \quad (1-R)\Omega_2 \quad (1-R)\Omega_3)^T . \tag{68}$$

Equations (65) and (68) are the main constraint equations used in the derivation of equations of motion which follows. Although they are approximate, the small angle approximations on which they are based are <u>very good</u> approximations.

<u>*Equations of Motion*</u>

Free-body diagrams of Bodies 1 and 2 are shown in Fig. 12. The forces $\underline{F}_P$ and $\underline{F}_Q$ are forces of constraint exerted by the launcher on the rocket, while $\underline{F}_R$ is the force exerted on Body 1 by Body 2. By letting $\underline{H}_{j/C_j}$ and $m_j \dot{\underline{R}}_{C_j}$ denote the rotational angular momentum and linear momentum, respectively, of Body j and referring to Fig. 12, we may write

$$\dot{\underline{H}}_{1/C_1} = \underline{\ell}_1 \times \underline{F}_R - \underline{r}_1 \times \underline{F}_P + \underline{T}_{1/2} + \underline{T}_s , \tag{69a}$$

$$\dot{\underline{H}}_{2/C_2} = \underline{\ell}_2 \times \underline{F}_Q + \underline{r}_2 \times \underline{F}_R - \underline{T}_{1/2} , \tag{69b}$$

$$m_1 \ddot{\underline{R}}_{C_1} = \underline{F}_T + m_1 \underline{g} + \underline{F}_P + \underline{F}_R \tag{69c}$$

and

$$m_2 \ddot{\underline{R}}_{C_2} = \underline{F}_Q = \underline{F}_R + m_2 \underline{g} \tag{69d}$$

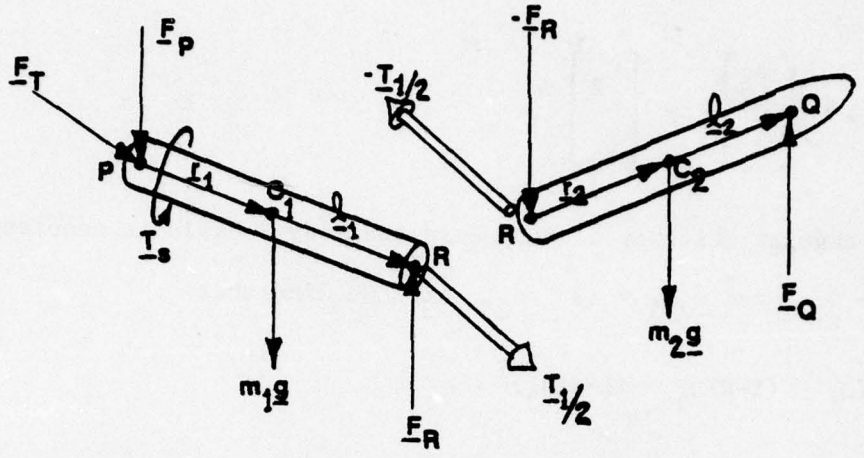


Figure 12. Free-body diagrams of bodies 1 and 2.

Equations (69c) and (69d) may be solved for $-\underline{F}_P$ and $\underline{F}_Q$, i.e.,

$$-\underline{F}_P = -m_1\ddot{\underline{R}}_{C_1} + \underline{F}_T + m_1\,\underline{g} + \underline{F}_R \tag{70a}$$

and

$$\underline{F}_Q = m_2\ddot{\underline{R}}_{C_2} + \underline{F}_R - m_2\,\underline{g}\ . \tag{70b}$$

Equations (70) may then be used to eliminate $\underline{F}_P$ and $\underline{F}_Q$ from the first two of Eqs. (69), viz.,

$$\dot{\underline{H}}_{1/C_1} = (\underline{\ell}_1+\underline{r}_1) \times \underline{F}_R - \underline{r}_1 \times m_1\,\ddot{\underline{R}}_{C_1} + \underline{r}_1 \times m_1\,\underline{g} + \underline{T}_{1/2} + \underline{T}_s + \underline{r}_1 \times \underline{F}_T \tag{71a}$$

and

$$\dot{\underline{H}}_{2/C_2} = (\underline{\ell}_2 + \underline{r}_2) \times \underline{F}_R + \underline{\ell}_2 \times m_2\ddot{\underline{R}}_{C_2} - \underline{\ell}_2 \times m_2\,\underline{g} - \underline{T}_{1/2}\ . \tag{71b}$$

Also, by adding the last two of Eqs. (69), we obtain

$$M \ddot{\underline{R}}_L = \underline{F}_T + M \underline{g} + \underline{F}_P + \underline{F}_Q , \tag{72}$$

where as before $M=m_1+m_2$ and $\ddot{\underline{R}}_C$ is the acceleration of the system center of mass. If we neglect the frictional forces which act parallel to the $x_L$-axis at P and Q, then

$$M \ddot{x}_{L_c} = \underline{F}_T \cdot \hat{\underline{i}}_L + M \underline{g} \cdot \hat{\underline{i}}_L \tag{73}$$

Letting $\underline{F}_R = F_{R_1} \hat{\underline{i}}_1 + F_{R_2} \hat{\underline{j}}_1 + F_{R_3} \hat{\underline{k}}_1$ and using the small angle approximation to $\underline{\underline{A}}$ to get

$$\underline{\ell}_2 + \underline{r}_2 \simeq (\ell_2+r_2)[\hat{\underline{i}}_1 + \theta_1 \hat{\underline{j}}_1 - \dot{\theta}_2 \hat{\underline{k}}_1] , \tag{74}$$

we may combine Eqs. (71) to get

$$\begin{aligned} \dot{\underline{H}}_{1/C_1} \simeq\ & [1/(R-1)]\dot{\underline{H}}_{2/C_2} + (\ell_1+r_1)F_{R_1}(\theta_2 \hat{\underline{j}}_1 + \theta_3 \hat{\underline{k}}_1) \\ & -[1/(R-1)][\underline{\ell}_2 \times (m_2 \ddot{\underline{R}}_{C_2} - m_2 \underline{g})] \\ & - \underline{r}_1[m_1 \ddot{\underline{R}}_{C_1} - m_1 \underline{g}] + [R/(R-1)]\underline{T}_{1/2} + \underline{T}_s \end{aligned} \tag{75}$$

At this point, we begin the change to matrix notation and express $\ddot{\underline{R}}_{C_1}$ and $\ddot{\underline{R}}_{C_2}$ in their Body 1-basis forms,†

---

†The brackets with subscripts indicate that the inertial, or total, vector derivative bracketed is evaluated in the basis corresponding to the subscript.

$$[\ddot{\underline{R}}_{C_1}]_1 = \underline{\underline{B}}(\ddot{x}_P \quad 0 \quad 0)^T + \underline{\tilde{\Omega}}\underline{\tilde{\Omega}}\underline{r}_1 - \underline{r}_1 \dot{\underline{\Omega}} \tag{76a}$$

and

$$[\ddot{\underline{R}}_{C_2}]_1 = \underline{\underline{B}}(\ddot{x}_P \quad 0 \quad 0)^T + \underline{\tilde{\Omega}}\underline{\tilde{\Omega}}(\underline{\ell}_1+\underline{r}_1) - (\underline{\tilde{\ell}}_1+\underline{\tilde{r}}_1)\dot{\underline{\Omega}}$$
$$+ \underline{\underline{A}}^T \underline{\tilde{\omega}}\underline{\tilde{\omega}}\, \underline{r}_2 - \underline{\underline{A}}^T \underline{\tilde{r}}_2 \dot{\underline{\omega}} \quad . \tag{76b}$$

Now, from Newton's second law, still using vectors,

$$\ddot{\underline{R}}_C = \underline{F}_T/M + \underline{g} \tag{77}$$

and, from kinematics and the definition of the center of mass,

$$M\ \ddot{\underline{R}}_C = M(\ddot{\underline{R}}_P + \ddot{\underline{r}}_1) + m_2(\ddot{\underline{\ell}}_1 + \ddot{\underline{r}}_2). \tag{78}$$

Thus, by expressing the derivatives of the vectors in Eq. (78) in the launcher basis using Eqs. (76), we get

$$(\ddot{x}_P \quad 0 \quad 0)^T_L = \underline{\underline{E}}_1 \underline{\underline{B}}^T \{\underline{F}_T/M - \underline{\tilde{\Omega}}\underline{\tilde{\Omega}}\underline{r}_1 + \underline{\tilde{r}}_1 \dot{\underline{\Omega}}$$
$$-\mu[(\underline{\tilde{\Omega}}\underline{\tilde{\Omega}}\ \underline{\ell}_1 - \underline{\tilde{\ell}}_1 \dot{\underline{\Omega}}) + \underline{\underline{A}}^T(\underline{\tilde{\omega}}\underline{\tilde{\omega}}\ \underline{r}_2 + (R-1)\underline{\tilde{r}}_2 \dot{\underline{\Omega}}]$$
$$+ \underline{\underline{C}}(0 \quad 0 \quad g)^T\}, \tag{79}$$

where we have used the constraint equation (68) to write $\dot{\underline{\omega}} = (\dot{\Omega}_1 \quad (1-R)\dot{\Omega}_2 \quad (1-R)\dot{\Omega}_3)^T$ and $\underline{r} = (r_2 \quad 0 \quad 0)^T$ has been assumed, also

$$\underline{\underline{E}}_1 = \begin{bmatrix} 1 & 0 & 0 \\ 0 & 0 & 0 \\ 0 & 0 & 0 \end{bmatrix}.$$

We next use Eqs. (76) and Eq. (79) in Eq. (78), expressed in matrix form, to obtain the equation which governs the rotational motion of Body 1,

$$
\begin{aligned}
\underline{\underline{L}}_{ON}\,\dot{\underline{\Omega}}_1 = &-\tilde{\underline{\Omega}}_1\,\underline{\underline{I}}_1\,\underline{\Omega}_1 + \underline{\underline{A}}^T\,\tilde{\underline{\omega}}_2\,\underline{\underline{I}}_2\,\underline{\omega}_2[1/(R-1)] \\
&-\mu(\ell_1+r_1)(F_T - M\ g\ \sin\theta_L)(0\quad \theta_2\quad \theta_2)^T \\
&- m_2[1/(R-1)]\underline{\underline{A}}^T\,\tilde{\underline{\ell}}_2\,\{\underline{\underline{A}}[\underline{\underline{B}}\,\underline{\underline{E}}_1\,\underline{\underline{B}}^T(\underline{F}_T/M - \tilde{\underline{\Omega}}_1\tilde{\underline{\Omega}}_1\,\underline{r}_1 \\
&- \mu(\tilde{\underline{\Omega}}_1\tilde{\underline{\Omega}}_1\underline{\ell}_1 + \tilde{\underline{\omega}}_2\tilde{\underline{\omega}}_2\,\underline{r}_2) + \underline{\underline{C}}(0\quad 0\quad g)^T \\
&+ \tilde{\underline{\Omega}}_1\tilde{\underline{\Omega}}_1(\underline{\ell}_1+\underline{r}_1)] + \tilde{\underline{\omega}}_2\tilde{\underline{\omega}}_2\,\underline{r}_2 - \underline{\underline{A}}\,\underline{\underline{C}}(0\quad 0\quad g)^T\} \\
&- m_1\,\tilde{\underline{r}}_1\,\underline{\underline{B}}\,\underline{\underline{E}}_1\,\underline{\underline{B}}^T\,[\underline{F}_T/M - \tilde{\underline{\Omega}}_1\tilde{\underline{\Omega}}_1\,\underline{r}_1 \\
&- \mu(\tilde{\underline{\Omega}}_1\tilde{\underline{\Omega}}_1\,\underline{\ell}_1 + \underline{\underline{A}}^T\,\tilde{\underline{\omega}}_2\tilde{\underline{\omega}}_2\,\underline{r}_2) + \underline{\underline{C}}(0\quad 0\quad g)^T] \\
&- m_1[\tilde{\underline{r}}_1\,\tilde{\underline{\Omega}}_1\tilde{\underline{\Omega}}_1\,\underline{r}_1 - \tilde{\underline{r}}_1\,\underline{\underline{C}}\,(0\quad 0\quad g)^T] \\
&+ [R/(R-1)]\underline{\underline{A}}(0\quad k_1\theta_2 + c\,\dot{\theta}_2\quad k\,\theta_3 + c\,\dot{\theta}_3)^T \\
&+ (T_s\quad 0\quad 0)^T\,, \qquad (80)
\end{aligned}
$$

where

$$
\begin{aligned}
\underline{\underline{L}}_{ON} = &\ \underline{\underline{I}}_1 + \underline{\underline{A}}^T\,\underline{\underline{I}}_2\,\underline{\underline{A}} - m_1[\tilde{\underline{r}}_1\tilde{\underline{r}}_1 - \tilde{\underline{r}}_1\,\underline{\underline{B}}\,\underline{\underline{E}}_1\,\underline{\underline{B}}^T\,\tilde{\underline{r}}_1] \\
&- [1/(R-1)]\ m_2\{[\underline{\underline{A}}^T\,\tilde{\underline{\ell}}_2\,\underline{\underline{A}}(\tilde{\underline{\ell}}_1+\tilde{\underline{r}}_1)] \\
&- \underline{\underline{A}}^T\,\tilde{\underline{\ell}}_2\,\underline{\underline{A}}\,\underline{\underline{B}}\,\underline{\underline{E}}_1\,\underline{\underline{B}}^T[\tilde{\underline{r}}_1 + \mu(\tilde{\underline{\ell}}_1 - \underline{\underline{A}}^T\,\tilde{\underline{r}}_2[1/(R-1)]) \\
&-(m_1/m_T)\,\tilde{\underline{r}}_1\,\underline{\underline{B}}\,\underline{\underline{E}}_1\,\underline{\underline{B}}^T(\underline{\ell}_1 - \underline{\underline{A}}^T\,\tilde{\underline{r}}_2[1/(R-1)])\}\} \qquad (81)
\end{aligned}
$$

and the axial component of $\underline{F}_R$, $F_{R_1}$, is approximated by $\mu(F_T - M\ g\ \sin\theta_L)$.

Numerical integrations of Eqs. (66), (79) and (80) can be accomplished via digital computer, using Eqs. (65) and (67) to compute $\theta_2$, $\theta_3$ and their time derivatives when required.

## 2.7 Results for Motion on a Rigid Launcher

As an example of the results which may be obtained by numerically integrating the on-launcher equations of motion, the solutions for $\Theta_N$ and $\Psi_N$ as functions of time for the GEM #7 model are given in Figs. 13 and 14. To be noted is that the initial value of $\Theta_N$, which is due to the bending of the rocket caused by its weight, is small in magnitude. As the thrust is applied and the rocket spins up (an eroding spin turbine is simply modeled by using $T_s = 0.02\ F_T$), the pitch angle of the nose oscillates about a mean value of about $8.8 \times 10^{-5}$ radians with damping apparent. The transfer of bending into the yaw plane through the Coriolis and Euler acceleration terms is also apparent in Fig. 14.

An important fact that requires further study is that the bending due to gravity and thrust is not as large in magnitude as that observed in certain flight tests; for example, those of GEM #7.

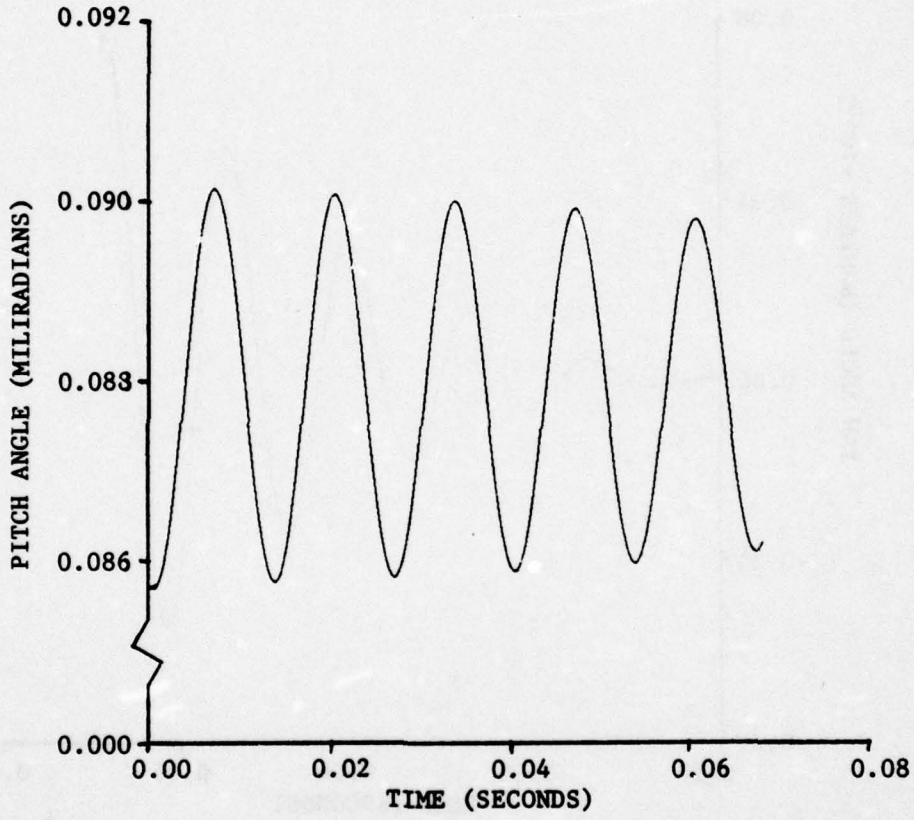


Figure 13. Theoretical attitude of rocket's nose during launch - pitch angle.

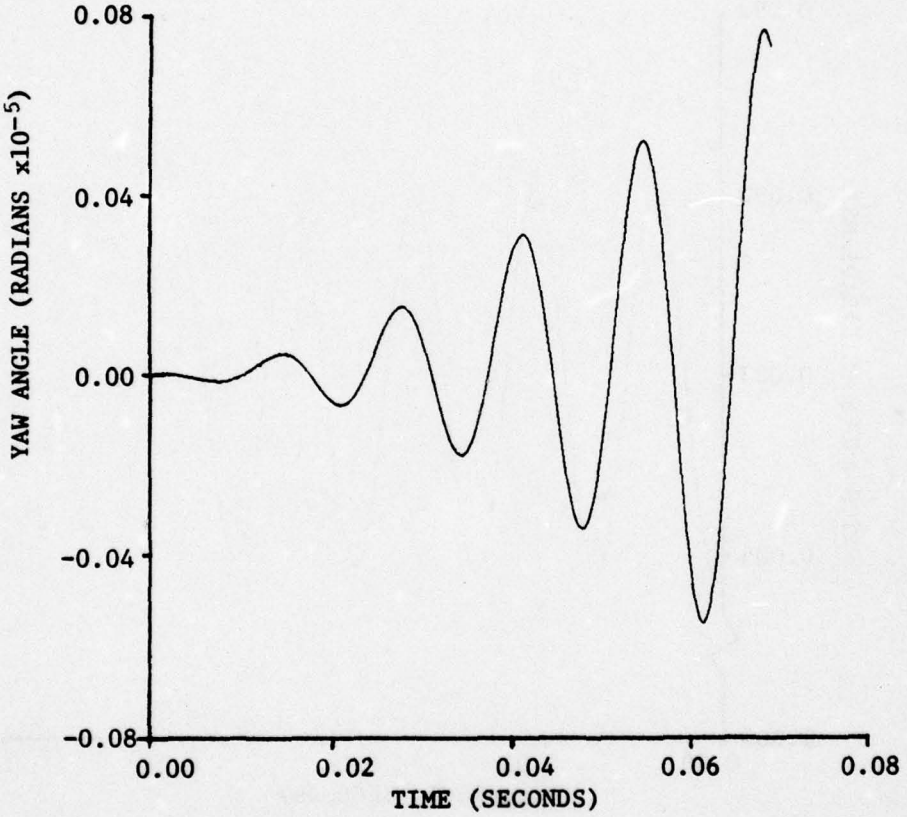


Figure 14. Theoretical attitude of rocket's nose during launch - yaw angle.

## SECTION 3. CONTINUOUS ROCKET MODEL

### 3.1 Description of the Model

The continuous rocket model developed during this study is an extension of that described in Ref. 9.[†] The Ref. 9 model is that of a pinned-pinned-free slender beam, which has its points of support constrained to move in a fixed straight line during launch and free to move during free-flight. The results obtained using this pinned-pinned-free model did not agree very well with optical lever data. Hence, the present model was conceived.

The continuous model actually is two models in the sense that during on-the-launcher motions of the rocket, its bending deformations are described using mode shapes for a pinned-pinned-free, uniform, slender beam, as in the previous model. However, during free-flight motion of the rocket, its bending is modeled using free-free mode shapes for a uniform, slender beam. The use of these mode shapes in the equations of motion presented here is not necessary, since mode shapes obtained experimentally, or, for example, by using finite element computer codes, could be used. In the absence of such mode shapes, however, these approximate ones were used to obtain results given later in this section.

Sketches of the physical model of the rocket during the launch phase, when two points of the rocket (points P and Q) are constrained to travel in a fixed straight line, and during the free-flight phase when the rocket's motion is unconstrained are shown in Fig. 15. The rocket is assumed to be a linearly

[†]A number of misprints are present in Ref. 9. A corrected copy can be obtained from the first author of this report upon request.

elastic body in the sense that it may deform transversely; however, it is assumed to be rigid longitudinally. A small segment of the rocket, obtained by cutting it transversely at two closely neighboring longitudinal stations is considered to have symmetric elastic properties, but the stiffness and mass density of the rocket may be functions of longitudinal position.

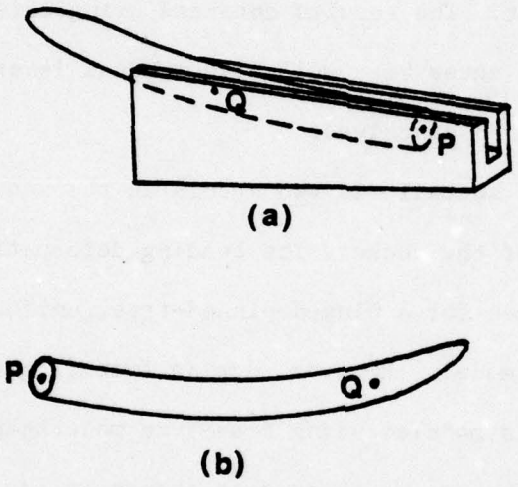


Figure 15. Sketches of continuous rocket model, (a) on launcher, (b) off launcher.

The mass of the rocket is assumed to be constant, although the thrust force which is assumed to act on it is generated by the mass flow of burned propellant from it. This assumption appears justified if the model is used in modeling motion of a rocket during only, say, the first second of its flight, provided its mass changes by only a small percentage during that time period.

Only the external force due to gravity, an "external" force and moment due to thrust and, during the on-launcher motion, constraint forces are assumed to be present. The thrust force is assumed to act at the front end of the "motor section" of the rocket as shown in Fig. 16 in determining the internal force due to thrust. However, for the purpose of computing the force and torque on the rocket due to thrust misalignment, the thrust is assumed to act on the aft end of the rocket. These assumptions are compatible, since the misalignment torques and forces are generated by undesirable turning of the flow from the motor due to the rocket's nozzle not being perfectly aligned mechanically with the rocket's longitudinal axis and to the rocket's bent shape, while the principal axial force should be considered to act at the front end of the motor section.[8]

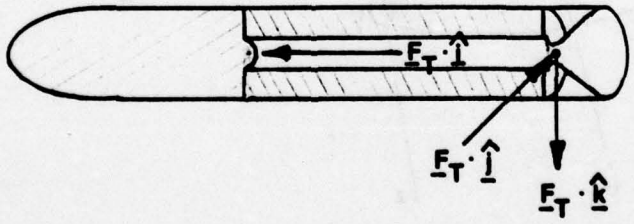


Figure 16. Positioning of the thrust force.

In Fig. 17, three coordinate frames used in developing equations of motion are shown. The OXYZ frame is fixed to the launcher and is assumed to be an inertial ("rigid" launcher) frame. The Pxyz frame has its origin at the aft end of the rocket with its x-axis passing through the point Q. It rotates in roll with the rocket. The $Cu_1u_2u_3$ frame has its origin at the

center of mass of the rocket and the $u_j$-axes are instantaneous, centroidal, principal axes of the rocket. The Pxyz system is of principal importance during the launch phase, since then the points P and Q are constrained to move in a straight line. During the free-flight phase, the $Cu_1u_2u_3$ system is used as the reference frame with respect to which bending deformations are measured because the equations of motion are thereby simplified and because the free-free mode shapes of a uniform beam due to transverse bending may be logically measured with respect to such a frame. Because different coordinate frames are used for the launch and free-flight phases, coordinate transformations between the frames are needed. These are discussed following derivations of the required equations of motion for each phase.

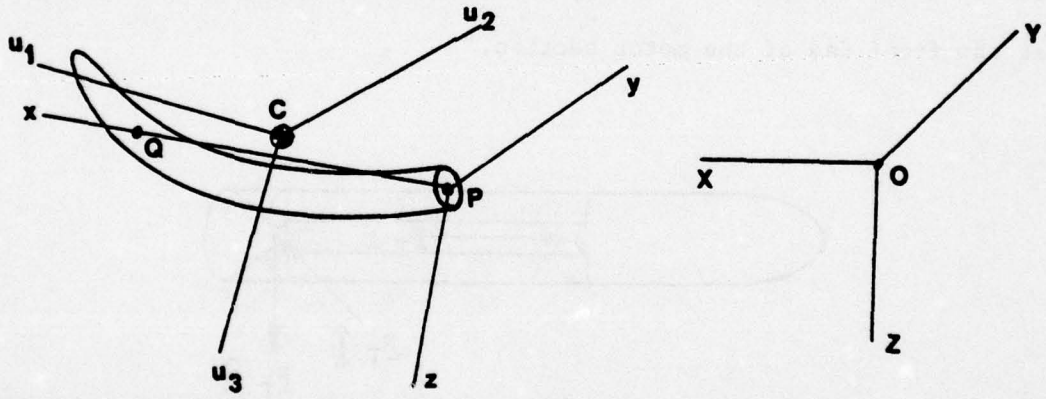


Figure 17. Coordinate frames used in analysis of continuous model.

We should point out that in this section some of the same symbols used in Section 2 are used in referring to <u>different</u> physical quantities than before. Hence, each section should be considered separately.

## 3.2 On-Launcher Motion

For motion during the launch phase, we need to determine the motion of the Pxyz system and the motion of the rocket relative to that system. To do

this, we consider the arbitrary rocket element of length $\Delta x$ shown in Fig. 18. In that figure, $\underline{r}(x)$ is the position of the aft end of the element with respect to point P, $-\underline{f}(x)$ is the internal[†] force acting on the -x-end of the rocket element and $-\underline{m}(x)$ is the moment on that end. The vectors $\underline{r}_a$ and $\underline{r}_b$ locate the centroids of the -x- and +x-ends, points a and b, respectively. The mass per unit length of the rocket is $\sigma(x)$ and $\sigma(x)\underline{g}\Delta x$ is the gravitational force on the element. As shown, the force and moment on the +x-end of the element are obtained from those on the -x-end by reversing their senses appropriately and using the first two terms of the Taylor series expansions of the resulting force $\underline{f}(x)$ and moment $\underline{m}(x)$ about x.

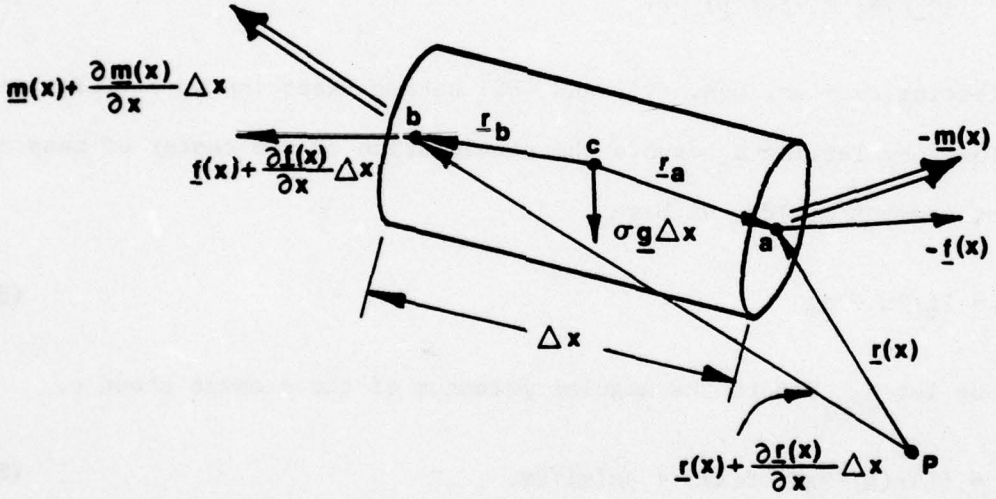


Figure 18. Forces and moments on a rocket segment.

The vectors $\underline{r}_a$ and $\underline{r}_b$ may be approximated by

$$\underline{r}_a \simeq -(\partial \underline{r}/\partial_x)\Delta x/2 \tag{82a}$$

and

$$\underline{r}_b = (\partial \underline{r}/\partial x)\Delta x/2, \tag{82b}$$

---

[†]This force is defined in Appendix A.

respectively. And, since the moment about c is given by

$$\underline{m}_c \simeq \underline{r}_a \times(-\underline{f}(x)) + \underline{r}_b \times(\underline{f}(x) + \partial\underline{f}(x)/\partial x\, \Delta x) + \partial\underline{m}(x)/\partial x\, \Delta x\ , \tag{83}$$

through first order in $\Delta x$,

$$\underline{m}_c \simeq \{[(\partial\underline{r}(x)/\partial x) \times \underline{f}(x)] + \partial\underline{m}(x)/\partial x\}\Delta x. \tag{84}$$

The net force, $\underline{f}_c$, on the element can also be approximated by

$$\underline{f}_c \simeq [(\partial\underline{f}/\partial x) + \sigma(x)\ \underline{g}]\ \Delta x, \tag{85}$$

By letting $\Delta x \to dx$, Eqs. (84) and (85) become exact in the differential sense. Then, by letting $\underline{a}_c$ denote the acceleration of the center of mass of the rocket segment $\sigma(x)dx$, we have

$$\sigma\underline{a}_c = \partial\underline{f}/\partial x + \sigma\underline{g}\ . \tag{86}$$

Also, if we let $\underline{h}_{dm}$ denote the angular momentum of the element about c,

$$\dot{\underline{h}}_{dm} = [(\partial\underline{r}(x)/\partial x) \times \underline{f}(x)] + \partial m(x)/\partial x. \tag{87}$$

Now, we may write $\underline{r}(x)$ as

$$\underline{r}(x) = x\ \hat{\underline{i}} + y(x)\ \hat{\underline{j}} + z(x)\ \hat{\underline{k}}\ , \tag{88}$$

so that,

$$\partial r(x)/\partial x = \hat{\underline{i}} + \partial y/\partial x\ \hat{\underline{j}} + \partial z/\partial x\ \hat{\underline{k}}\ . \tag{89}$$

We next differentiate Eq. (87) with respect to x and use Eqs. (86) and (89) to obtain the result,

$$\partial \dot{\underline{h}}_{dm}/\partial x = + \partial[(\partial y/\partial x\ \hat{\underline{j}} + \partial z/\partial x\ \hat{\underline{k}})\ x\ \underline{f}(x)]/\partial x$$

$$+ [\hat{\underline{i}}\ x\ (\sigma \underline{a}_c - \sigma\ \underline{g}) + \sigma^2\ \underline{m}(x)/\partial x^2] \tag{90}$$

At this point we chose to write y and z as $y = y_o(x) + \eta(x,t)$ and $z = z_o(x) + \zeta(x,t)$, respectively, where $y_o(x)$ and $z_o(x)$ are "permanent" displacements of c from the x-axis. These are due to non-straightness of the rocket. Also, $\eta$ and $\zeta$ are displacements due to elastic deformation of the rocket. Furthermore, we express $\underline{h}_{dm}$ explicitly as

$$\underline{h}_{dm} = \underline{dj}\ \underline{\omega}_{dm}\ , \tag{91}$$

where $\underline{dj}$ is the inertia dyadic of the segment $\sigma\ dx$ and $\underline{\omega}_{dm}$ is its total angular velocity. Moreover, we let $\underline{\Omega}$ denote the angular velocity of the Pxyz reference frame, let the unit vector triads $(\hat{\underline{i}}_L, \hat{\underline{j}}_L, \hat{\underline{k}}_L)$, $(\hat{\underline{i}}, \hat{\underline{j}}, \hat{\underline{k}})$ and $(\hat{i}', \hat{j}', \hat{k}')$ be associated with the launcher-fixed frame $Ox_Ly_Lz_L$, the Pxyz frame and a reference frame fixed in mass segment dm, respectively, and let subscripts L and m denote the launcher and segment bases, respectively, while no subscript implies that the Pxyz basis is used. Then, we may write

$$\underline{h}_{dm} = \underline{dj}_m(\underline{\Lambda}\ \underline{\Omega} + \underline{\lambda}_m)\ , \tag{92}$$

where

$$\underline{\Lambda} = \begin{bmatrix} 1 & \theta_3 & -\theta_2 \\ -\theta_3 & 1 & 0 \\ \theta_2 & 0 & 1 \end{bmatrix}\ , \tag{93a}$$

$$\theta_2 = -(\partial\zeta/\partial x + \partial z_o/\partial x), \tag{93b}$$

$$\theta_3 = \partial\eta/\partial x + \partial y_o/\partial x, \tag{93c}$$

$$\underline{\Omega} = (\Omega_x \quad \Omega_y \quad \Omega_z)^T, \tag{93d}$$

$$\underline{\lambda}_m = (0 \quad \dot{\theta}_2 \quad \dot{\theta}_3)^T, \tag{93e}$$

$$\dot{\theta}_2 = -\partial^2\zeta/\partial x\partial t \tag{93f}$$

and

$$\dot{\theta}_3 = \partial^2\eta/\partial x\partial t . \tag{93g}$$

It follows therefore, from (vector notation) $\dot{\underline{h}}_{dm} = (\delta\underline{h}_{dm}/\delta t)_m + (\underline{\Omega}+\underline{\lambda})x\ \underline{h}_{dm}$ and Eq. (87), that

$$\underline{\underline{dj}}(\underline{\underline{\Lambda}}\ \underline{\Omega} - \underline{\tilde{\lambda}}_m\ \underline{\underline{\Lambda}}\ \underline{\Omega} + \underline{\dot{\lambda}}_m) + (\underline{\underline{\Lambda}}\ \underline{\Omega} + \underline{\lambda}_m)\underline{\underline{dj}}(\underline{\underline{\Lambda}}\ \underline{\Omega} + \underline{\lambda}_m)$$

$$= + \underline{\underline{\Lambda}}[(\partial\underline{r}(x)/\partial x)\ \underline{f}(x) + \partial\underline{m}(x)/\partial x] . \tag{94}$$

The acceleration $\underline{a}_c$ may also be expressed in the matrix form,

$$\underline{a}_c = \underline{\underline{B}}\ \ddot{\underline{R}}_{\underline{L}p} + 2\ \tilde{\underline{\Omega}}\ \dot{\underline{r}} + \tilde{\underline{\Omega}}\ \tilde{\underline{\Omega}}\ \underline{r} - \tilde{\underline{r}}\ \dot{\underline{\Omega}} + \ddot{\underline{r}} , \tag{95}$$

where

$$\underline{\underline{B}} = \begin{bmatrix} 1 & 0 & 0 \\ 0 & c\phi & s\phi \\ 0 & -s\phi & c\phi \end{bmatrix} , \tag{96}$$

$\ddot{\underline{R}}_{\underline{L}p}$ is the acceleration of point P, $\dot{\underline{r}} = (0 \quad \partial\eta/\partial t \quad \partial\zeta/\partial t)^T$ and $\ddot{\underline{r}} = (0 \quad \partial^2\eta/\partial t^2 \quad \partial^2\zeta/\partial t^2)^T$ .

Using Eqs. (94) and (95) in Eq. (90) and neglecting the moments due to components† of $\underline{f}(x)$ other than the axial one, which we now call $f(x)$, we get

$$\frac{\partial}{\partial x}\{\underline{\Lambda}^T \underline{\underline{dj}}(\underline{\Lambda}\,\underline{\Omega} - \underline{\tilde{\lambda}}\,\underline{\Lambda}\,\underline{\Omega} + \underline{\dot{\lambda}}) + \underline{\Lambda}^T(\underline{\Lambda}\,\underline{\Omega} + \underline{\lambda})\underline{\underline{dj}}(\underline{\Lambda}\,\underline{\Omega} + \underline{\lambda})\}$$

$$+ \frac{\partial}{\partial x}(0 \quad \theta_2 f(x) \quad \theta_3 f(x))^T + \partial^2 \underline{m}(x)/\partial x^2$$

$$- (0 \quad \sigma a_{c_z} \quad -\sigma a_{c_y})^T + (0 \quad f_{g_z} \quad -f_{g_y})^T = \underline{0}\,, \tag{97}$$

where $a_{c_y}$ and $a_{c_z}$ are the y- and z-components, respectively, of the acceleration of c and $f_{gy}$ and $f_{gz}$ are analogous components of $\sigma\underline{g}$. The term in curly brackets is the time rate of change of the rotational angular momentum of the rocket element about its center of mass. If the rocket has an <u>essentially</u> uniform mass distribution and is very slender, this term should vary little with position x. Hence, to simplify matters considerably, we neglect the partial derivative of the bracketed term with respect to x. We then use the fact that on the launcher $\underline{\Omega} = (\Omega_x \quad 0 \quad 0)^T$ and also use Euler's bending moment equation to obtain the following equations which govern the bending of the rocket while it is on the launcher:

$$\sigma[\ddot{\eta} - 2\Omega_x\dot{\zeta} - \dot{\Omega}_x(x_o+\zeta) - \Omega_x^2(y_o+\eta)]$$

$$-[(y_o' + \eta')\, f(x)]' - f_{gy} + (E\,I\,\eta'')'' = 0 \tag{98a}$$

$$\sigma[\ddot{\zeta} + 2\Omega_x\dot{\eta} + \dot{\Omega}_x(y_o+\eta) - \Omega_x^2(z_o+\zeta)]$$

$$-[(z_o' + \zeta')\, f(x)]' - f_{gz} + (E\,I\,\zeta'')'' = 0, \tag{98b}$$

---

†The force $\underline{f}(x)$, as defined in Appendix A, has a transverse component only when x=0.

where $(\dot{})\triangleq\partial(\ )/\partial t$ and $(\ )'\triangleq\partial(\ )/\partial x$.

Equations (98) are subject to the following boundary conditions:

At point P:

Zero Deflection

$$\eta = \zeta = 0 \qquad \text{(2 conditions)}$$

Zero Moment

$$\eta'' = \zeta'' = 0. \qquad \text{(2 conditions)}$$

At the nose of the rocket, x = L:

Zero Moment

$$\eta'' = \zeta'' = 0 \qquad \text{(2 conditions)}$$

Zero Shear

$$(E\ I\ \eta'')' = (E\ I\ \zeta'')' = 0. \qquad \text{(2 conditions)}$$

Also, at the point Q, $\eta$ and $\zeta$ must be zero (continuous) and have continuous first derivatives with respect to x. These are four more conditions.

The equations which govern the rocket's center of mass and its rotation about its center of mass while it is on the launcher may be obtained from Equations (86) and (87), by integrating those equations over the length of the rocket. From Eq. (86), we have

$$\int_{M_T}\sigma\underline{a}_c\,dx = \int_0^{x_{M^-}}\partial\underline{f}(x)/\partial x\,dx + \int_{x_{M_+}}^{L}\partial\underline{f}(x)/\partial x\,dx + \int_0^L\sigma\underline{g}\,dx, \qquad (99)$$

where the integral over $\partial f(x)/\partial x$ has been broken into two pieces to allow for the discontinuity in $\underline{f}(x)$ at $x=x_M$. Now, the left-hand side of this equation is the total mass $M_T$ times the acceleration of the center of mass $\underline{a}_C$. Also,

neglecting any frictional forces at P and Q and referring to the definitions of f(x) given in Appendix A, we get,

$$M_T \underline{a}_C = \underline{F}_T + M_T \underline{g} . \tag{100}$$

We are concerned, during the launch phase, with only motion along the $x_L$-axis. Hence, we need only the $x_L$-component of Eq. (100). This can be written as

$$M_T \dot{u}_{L_p} = F_T - M_T g \sin \Theta_L , \tag{101}$$

where $u_{L_p}$ is the $x_L$-component of the velocity of P and $\Theta_L$ is the launcher elevation angle.

While it is on the launcher, the rotation of the rocket is constrained in such a manner that only rotation of the Pxyz frame about the x-axis is allowed. Although the bending of the rocket produces variations in the moment of inertia about the x-axis they are very small compared to the axial moment of inertia of the undeformed rocket. Thus, letting $T_x$ denote the x-component of the external torque acting on the rocket.

$$\dot{\Omega}_x = T_x / I_x . \tag{102}$$

In addition to the Eqs. (101) and (102) the kinematic equations,

$$\dot{x}_{L_p} = u_{L_p} \tag{103a}$$

and

$$\dot{\phi} = \Omega_x , \tag{103b}$$

are needed.

Equations (101) through (103) are uncoupled from Eqs. (98). The latter are partial differential equations with time varying coefficients and apparently can only be solved exactly by using finite difference techniques. Alternatively, approximate solutions to Eqs. (98) may be obtained by obtaining a set of ordinary differential equations using the method of assumed modes.[10] This alternative approach is attractive and also produces accurate results if the mode shapes are chosen carefully and an adequate number of them is used.

The mode shapes chosen for use herein are those for the transverse vibration of a pinned-pinned-free, uniform, slender beam. These were also used in Ref. 9, but there they were used for both the launch phase and free-flight phases of motion, while here they are used only during the launch phase. How these mode shapes $\psi_j$ are determined is discussed in Appendix B. They are comparison mode shapes, in that they satisfy the geometric boundary conditions and also the conditions of zero bending moment at each end and zero shear at the nose of the rocket.

To transform Eqs. (98) into ordinary differential equations we approximate $\eta$ and $\zeta$ by

$$\eta = \sum_{j=1}^{N} p_j \psi_j \tag{104a}$$

and

$$\zeta = \sum_{j=1}^{N} q_j \psi_j , \tag{104b}$$

respectively, where the $p_j$ and $q_j$ are functions of time t and the $\psi_j$ are, of course, functions of x only. By substituting Eqs. (104) into Eqs. (98),

multiplying each of Eqs. (98) by $\psi_i$, integrating over the length of the rocket and performing a good bit of algebra, we obtain the matrix equations,

$$\underline{\underline{M}}(\ddot{\underline{p}} - 2\Omega_x \dot{\underline{q}} - \dot{\Omega}_x \underline{q} - \Omega_x^2 \underline{p}) + (\underline{\underline{K}} - F_T \underline{\underline{\Gamma}})\underline{p}$$

$$-(g \sin \Phi)\underline{m} + F_T \underline{c} - \dot{\Omega}_x \underline{b} - \Omega_x^2 \underline{a} + \underline{\underline{D}} \dot{\underline{p}} = \underline{0} \tag{105a}$$

$$\underline{\underline{M}}(\ddot{\underline{q}} + 2\Omega_x \dot{\underline{p}} + \dot{\Omega}_x \underline{p} - \Omega_x^2 \underline{q}) + (\underline{\underline{K}} - F_T \underline{\underline{\Gamma}})\underline{q}$$

$$-(g \cos \Phi)\underline{m} + F_T \underline{d} + \dot{\Omega}_x \underline{a} - \Omega_x^2 \underline{b} + \underline{\underline{D}} \dot{\underline{q}} = \underline{0} \tag{105b}$$

where $\underline{\underline{M}}$ is an NxN matrix with elements,

$$m_{ij} = \int_0^L \sigma \psi_i \psi_j \, dx \; ; \tag{106a}$$

$\underline{p}$ and $\underline{q}$ are Nxl matrices with elements $p_j$ and $q_j$, respectively; $\underline{\underline{K}}$ and $\underline{\underline{\Gamma}}$ are NxN matrices with elements,

$$k_{ij} = \int_0^L \psi_i (E \, I \, \psi_j'')'' \, dx \tag{106b}$$

and

$$\gamma_{ij} = \int_0^L \psi_j' \psi_i' \, f(x) \, dx \; , \tag{106c}$$

respectively; $\underline{m}$ is an Nxl matrix with elements,

$$m_i = \int_0^L \sigma \psi_i \, dx \; . \tag{106d}$$

Also, $\underline{a}$, $\underline{b}$, $\underline{c}$ and $\underline{d}$ are Nx1 matrices with elements,

$$a_i = \int_0^L \sigma \psi_i y_o \, dx \tag{106e}$$

$$b_i = \int_0^L \sigma \psi_i z_o \, dx \tag{106f}$$

$$c_i = \int_0^L \psi_i' y_o' f(x) \, dx \tag{106g}$$

and

$$d_i = \int_0^L \psi_i' z_o' f(x) \, dx \, , \tag{106h}$$

respectively. Finally $\underline{\underline{D}}$ is an NxN damping matrix. Equations (102) through (103) and (105) are the governing equations for the launch phase.

Since the principal type of attitude data available for free rockets is optical lever data and since the quantities measured are optical lever are the pitch and yaw angles of the nose of the rocket, we require expressions for these angles in terms of the roll angle $\Phi$ and the $p_j$ and $q_j$. Because the body-fixed angles the rocket's nose makes with the x-axis are $\theta_{2N}=-(\partial\zeta/\partial x)_{x=L}$ and $\theta_{3N}=(\partial\eta/\partial x)_{x=L}$. Hence,

$$\theta_{2N} \simeq -\sum_{j=1}^{N} \psi_j'(L) q_j \tag{107a}$$

and

$$\theta_{3N} \simeq \sum_{j=1}^{N} \psi_j'(L) p_j \, . \tag{107b}$$

These may be transformed into pitch and yaw angles $\Theta_N$ and $\Psi_N$ of the rocket's nose using the expressions,

$$\Theta_N = \Theta_L + \theta_{2N} \cos \Phi - \theta_{3N} \sin \Phi \tag{108a}$$

and

$$\Psi_N = \theta_{2N} \sin \Phi + \theta_{3N} \cos \Phi. \tag{108b}$$

## 3.3 Free Motion

In describing the free motion of the rocket, we switch to the coordinate frame $Cu_1u_2u_3$ which was defined previously. If the rotary inertia term $\partial \dot{\underline{h}}_{dm}/\partial x$ is again neglected and the internal force treated as before, the bending equations for the free-flight phase are

$$\begin{aligned} &-(E\ I\ u''_{2e})'' + [f(x)\ u'_2]' + \sigma \underline{g} \cdot \hat{\underline{e}}_2 + F_T\ (\theta_{3p} + \alpha_z)\ \delta(x-0) \\ &\quad = \sigma[\ddot{\underline{R}} \cdot \hat{\underline{e}}_2 + \ddot{u}_{2e} - 2\omega_1 \dot{u}_{3e} - \omega_1^2\ u_2 + \omega_2 \omega_1 u_1 \\ &\quad - \dot{\omega}_1\ u_3 + \dot{\omega}_3\ u_1] \end{aligned} \tag{109a}$$

and

$$\begin{aligned} &-[E\ I\ u''_{3e}]'' + [f(x) u'_3]' + \sigma \underline{g} \cdot \hat{\underline{e}}_3 + F_T\ (\theta_{2p} - \alpha_y)\ \delta(x-0) \\ &\quad = \sigma[\ddot{\underline{R}} \cdot \hat{\underline{e}}_3 + \ddot{u}_{3e} + 2\omega_1 \dot{u}_{2e} - \omega_1^2\ u_3 + \omega_3 \omega_1 u_1 \\ &\quad + \dot{\omega}_1 u_2 - \dot{\omega}_2 u_1]\ , \end{aligned} \tag{109b}$$

where $u_{2e}$ and $u_{3e}$ are elastic deformations in the $u_2$- and $u_3$-directions, $\hat{\underline{e}}_2$ and $\hat{\underline{e}}_3$ are unit vectors with the $u_2$- and $u_3$-axes, $\ddot{\underline{R}}_c$ is the acceleration of the center of mass of the rocket, $\omega_j$ is the $u_j$-component the angular

velocity of the $Cu_1u_2u_3$ coordinate frame and $\ddot{\underline{R}}_C$ is the acceleration of the center of mass of the rocket.

Now, since only the external forces of thrust and gravity are assumed to act on the rocket,

$$\ddot{\underline{R}}_C = \underline{F}_T/M_T + \underline{g} \ , \tag{110}$$

Hence, the gravity terms disappear from Eqs. (109) when Eq. (110) is used and we get

$$\sigma[\ddot{u}_{2e} - 2\,\omega_1\dot{u}_{3e} - \omega_1^2u_2 + \omega_1\omega_2u_1 - \dot{\omega}_1u_3 + \dot{\omega}_3u_1] + F_T(\theta_{3p} + \alpha_z)\,\delta(x-0)$$

$$= -[E\,I\,u_{2e}'']'' + [f(x)u_2']' - (\sigma/M_T)\underline{F}_T\cdot\hat{\underline{e}}_2 \tag{111a}$$

and

$$\sigma[\ddot{u}_{3e} + 2\omega_1\dot{u}_{2e} - \omega_1^2u_3 + \omega_1\omega_3u_1 + \dot{\omega}_1u_2 - \dot{\omega}_2u_2] + F_T\,(\theta_{2p} - \alpha_y)\,\delta(x-0)$$

$$= -[E\,I\,u_{3e}'']'' + [f(x)u_3']' - (\sigma/M_T)\underline{F}_T\cdot\hat{\underline{e}}_3 \ . \tag{111b}$$

As stated, the axes of the $Cu_1u_2u_3$ system are at all times the centroidal principal axes of the rocket. We shall use this fact now in deriving equations which govern the rocket's rotational motion.

The acceleration of the arbitrary element of mass dm of the rocket shown in Fig. 19 is

$$\ddot{\underline{r}}_{dm} = \ddot{\underline{R}}_C + \ddot{\underline{u}} + \ddot{\underline{\rho}} \ , \tag{112}$$

where $\underline{u}$ is, as before, a vector from C to a point c on the elastic axis and $\underline{\rho}$ is a vector from c to the mass element. The point c is also assumed to be the center of mass of segment of the rocket of length $du_1$.

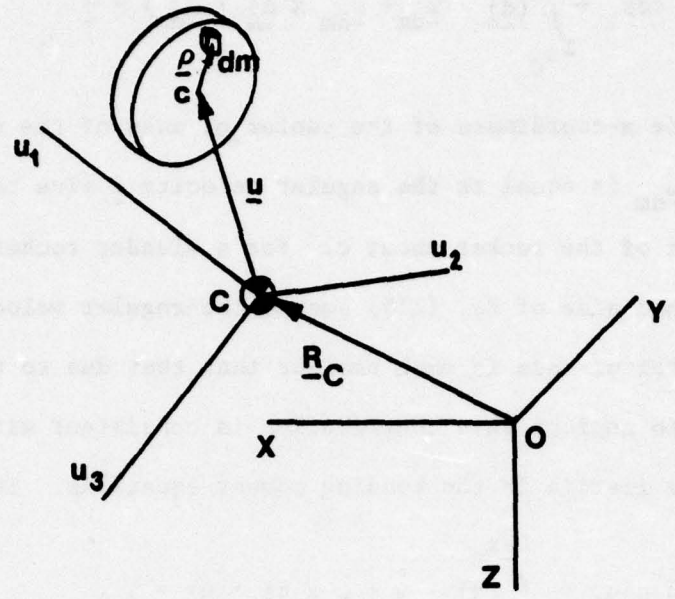


Figure 19. Mass element of flexible rocket.

Now, if the total external torque on the rocket about its center of mass is $\underline{T}$,

$$\int_{M_T} (\underline{u}+\underline{\rho}) \times \ddot{\underline{r}}_{dm} \, dm = \underline{T} \, , \tag{113}$$

and since $\ddot{\underline{R}}_c$ is independent of the integration, and $\underline{u} + \underline{\rho}$ is the vector from C to dm, we can reduce (113) to

$$\int_{M_T} (\underline{u}+\underline{\rho}) \times (\ddot{\underline{u}}+\ddot{\underline{\rho}}) \, dm = \underline{T} \, . \tag{114}$$

Because $\underline{u}$ depends only on $u_1$ (the "longitudinal" coordinate) we may integrate over the segment of the rocket of length $du_1$ to get†

†In this subsection, a small circle over a vector denotes the time derivative of that vector in the $Cu_1u_2u_3$ frame.

$$\int_{-x_C}^{L-x_C} \underline{u} \times \ddot{\underline{u}}\, \sigma du_1 + \int_{-x_C}^{L-x_C} (\underline{\underline{dj}} \cdot \dot{\underline{\omega}}_{dm} + \underline{\omega}_{dm} \times \underline{\underline{dj}} \cdot \underline{\omega}_{dm}) = \underline{T} \ , \tag{115}$$

where $x_C$ is the x-coordinate of the center of mass of the rocket in the Pxyz frame. Now, $\underline{\omega}_{dm}$ is equal to the angular velocity $\underline{\omega}$ plus the angular velocity of the segment of the rocket about c. For a slender rocket, the contribution to the left-hand side of Eq. (115) due to the angular velocity of the segment about its center of mass is much smaller than that due to the remaining terms. Furthermore, to neglect this contribution is consistent with the approximation of zero rotary inertia in the bending moment equations. Thus, we obtain

$$\int_{-x_C}^{L-x_C} \underline{u} \times \ddot{\underline{u}}\, \sigma du_1 + \int_{-x_C}^{L-x_C} (\underline{\underline{dj}} \cdot \dot{\underline{\omega}} + \underline{\omega} \times \underline{\underline{dj}} \cdot \underline{\omega}) \simeq \underline{T} \ . \tag{116}$$

Finally, we shall neglect the small terms in the second integral in Eq. (116) which are due to the rotation of the segment of the rocket with respect to the $Cu_1u_2u_3$ frame due to bending. This is also consistent with the assumption of a slender rocket.

Now,

$$\ddot{\underline{u}} = \mathring{\underline{u}}^{\circ} + 2\underline{\omega}x\mathring{\underline{u}} + \underline{\omega}x\underline{\omega}x\underline{u} + \dot{\underline{\omega}}x\underline{u} \ , \tag{117}$$

and because the $u_j$ axes are principal axes we can use results of that fact,

$$\int_{-x_C}^{L-x_C} \sigma u_i u_j \, du_1 = 0 \quad (i,j=1,2,3,i\neq j) \ , \tag{118a}$$

$$\int_{-x_C}^{L-x_C} \sigma u_1 \dot{u}_j \, du_1 = 0 \quad (j=2,3) \tag{118b}$$

and

$$\int_{-x_C}^{L-x_C} \sigma u_1 \ddot{u}_j \, du_1 = 0 \quad (j=2,3), \tag{118c}$$

to obtain from Eq. (116) the result,

$$\underline{\underline{I}}_C \cdot \dot{\underline{\omega}} + \underline{\omega} \times \underline{\underline{I}}_C \cdot \underline{\omega} = \underline{T} , \tag{119}$$

where $\underline{\underline{I}}_C$ is the centroidal, principal inertia dyadic. The elements of $\underline{\underline{I}}_C$ must, of course, differ slightly from the principal moments of inertia of a perfectly straight rocket, but such differences are second order in $u_{j0}^{\dagger}$ and/or $u_{je}$. Hence, they are neglected. It follows that the only way in which Eq. (119) can be affected by the bending of the rocket is through the torque $\underline{T}$.

The torque $\underline{T}$ is due to misalignment of the centerline of the nozzle with the the $u_1$-axis. As shown in Fig. 20, this misalignment is assumed due to three factors; the mechanical misalignment of the nozzle ($\alpha_y$ and $\alpha_z$), the non-straightness of the rocket [$P(\partial u_{30}/\partial u_1)_P$ and $(\partial u_{20}/\partial u_1)_P$] and the bending of the rocket [$(\partial u_{3e}/\partial u_1)_P$ and $(\partial u_{2e}/\partial u_1)_P$]. The torque is

$$\underline{T} = F_T \, x_C \left\{ [(\partial u_3/\partial u_1)_P - \alpha_y] \, \hat{e}_2 - [(\partial u_2/\partial u_1)_P + \alpha_z] \, \underline{\hat{e}}_3 \right\} . \tag{120}$$

---

$^{\dagger}$The $u_{j0}$ are the counterparts of $y_o$ and $z_o$.

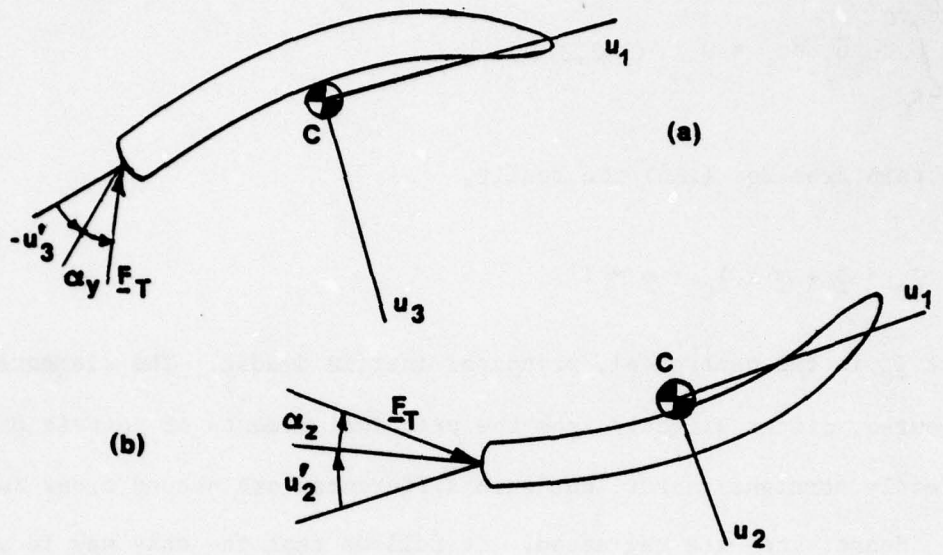


Figure 20. Orientation of thrust vector.

The translation of the center of mass of the rocket is governed by Eq. (110); however, we chose to rewrite it in the form,

$$\dot{\underline{V}} + \underline{\omega} \times \underline{V} = \underline{F}_T/M_T + \underline{g} \tag{121}$$

where $\underline{V}$ is the velocity of C with components u, v and w and

$$\underline{F}_T = F_T[\hat{\underline{e}}_1 + [(\partial u_2/\partial u_1)_P + \alpha_z]\ \hat{\underline{e}}_2 - [-(\partial u_3/\partial u_1)_P + \alpha_y]\ \hat{\underline{e}}_3] \ . \tag{122}$$

Finally, the kinematic equations for translational and rotational motion are the usual ones,

$$\begin{bmatrix} \dot{X}_C \\ \dot{Y}_C \\ \dot{Z}_C \end{bmatrix} = \begin{bmatrix} 1 & 0 & 0 \\ 0 & c\phi & s\phi \\ 0 & s\phi & c\phi \end{bmatrix} \begin{bmatrix} c\theta & 0 & -s\theta \\ 0 & 1 & 0 \\ s\theta & 0 & c\theta \end{bmatrix} \begin{bmatrix} c\psi & s\psi & 0 \\ -s\psi & c\psi & 0 \\ 0 & 0 & 1 \end{bmatrix} \begin{bmatrix} u \\ v \\ w \end{bmatrix} \tag{123}$$

and

$$\dot{\phi} = \omega_1 + (\omega_2 \, s\phi + \omega_3 \, c\phi)\tan\theta \tag{124a}$$

$$\dot{\theta} = \omega_2 \, c\phi - \omega_3 s\phi \tag{124b}$$

$$\dot{\psi} = (\omega_2 \, s\phi + \omega_3 c\phi)/\cos\theta, \tag{124c}$$

respectively.

Equations (111), (119), (121), (123) and (124) are those required to completely specify the bending of the rocket and the motion of its center of mass. However, we still must transform Eqs. (111) into ordinary differential equations if we are to solve those equations in the same manner as the launch-phase bending equations.

As stated at the first of this section, we shall use the mode shapes for a slender, uniform free-free beam to make the required transformation. The mode shapes are denoted $\phi_j$ and are functions of x. However, it is obvious that $u_1 = x - x_c$. They are discussed in Appendix C.

Proceeding as in the launch phase case, we set

$$u_{2e} \simeq \sum_{j=1}^{N} P_j \, \phi_j \tag{124a}$$

and

$$u_{3e} \simeq \sum_{j=1}^{N} Q_j \, \phi_j \quad , \tag{124b}$$

where the $P_j$ and $Q_j$ are time functions. By inserting these approximations into Eqs. (111), performing the necessary multiplications by $\phi_i$ and integrating over the length of the rocket, we get

$$\underline{\underline{M}}_f(\ddot{\underline{P}} - 2\,\omega_1\,\dot{\underline{Q}} - \dot{\omega}_1\underline{Q} - \omega_1^2\,\underline{P}) + (\underline{\underline{K}}_f - F_T\,\underline{\underline{\Gamma}}_f)\underline{P}$$

$$+ (\dot{\omega}_3 + \omega_1\omega_2)\underline{\ell}_f - \dot{\omega}_1\,\underline{b}_f - \omega_1^2\,\underline{a}_f + F_T\,\underline{c}_f - F_T(\theta_{3p}+\alpha_z)\underline{\phi}(0)$$

$$+ (F_T/M_T)_2\,\underline{m}_f = \underline{0} \tag{125a}$$

and

$$\underline{\underline{M}}_f(\ddot{\underline{Q}} + 2\,\omega_1\,\dot{\underline{P}} + \dot{\omega}_1\,\underline{P} - \omega_1^2\,\underline{Q}) + (\underline{\underline{K}}_f - F_T\,\underline{\underline{\Gamma}}_f)\underline{Q}$$

$$+(\omega_1\omega_3 - \dot{\omega}_2)\underline{\ell}_f + \dot{\omega}_1\,\underline{a}_f - \omega_1^2\,\underline{b}_f - F_T\,\underline{d}_f - F_T(\theta_{2p}-\alpha_y)\underline{\phi}(0)$$

$$+ (F_T/M_T)_3\,\underline{m}_f = 0\ , \tag{125b}$$

where the subscript f is used to indicate that the matrices so subscripted are for the free-flight phase. The matrix $\underline{\underline{M}}_f$ is NxN with elements

$$m_{ij_f} = \int_0^L \sigma\,\phi_i\phi_j\,dx\ . \tag{126a}$$

The matrices $\underline{P}$ and Q are Nx1 matrices with elements $P_j$ and $Q_j$, respectively. Also, the matrices $\underline{\underline{K}}_f$ and $\underline{\underline{\Gamma}}_f$ are NxN with elements,

$$k_{ij_f} = \int_0^L \phi_i(E\ I\ \phi_j'')''\,dx \tag{126b}$$

and

$$\gamma_{ij_f} = \int_0^L \phi_i'\phi_j'\ f(x)\,dx, \tag{126c}$$

respectively. Furthermore, the elements of the matrices $\underline{a}_f$, $\underline{b}_f$, $\underline{c}_f$, $\underline{d}_f$, $\underline{\ell}_f$ and $\underline{m}_f$ are defined as follows:

$$a_{i_f} = \int_0^L \sigma\phi_i\,u_{20}\,dx \tag{126d}$$

$$b_{i_f} = \int_0^L \sigma\phi_i \, u_{30} \, dx \, , \tag{126e}$$

$$c_{i_f} = \int_0^L \phi_i' \, u_{20}' \, f(x) \, dx \, , \tag{126f}$$

$$d_{i_f} = \int_0^L \phi_i' \, u_{30}' \, f(x) \, dx \, , \tag{126g}$$

$$\ell_{i_f} = \int_0^L \phi_i (x - x_c) \, dx \, , \tag{126h}$$

$$m_{i_f} = \int_0^L \phi_i \sigma \, dx \, , \tag{126i}$$

$$(F_T/M_T)_2 = (F_T/M_T)[u_{20}' + \sum_{j=1}^{N} P_j \phi_j'(0) + \alpha_z] \tag{126j}$$

and

$$(F_T/M_T)_3 = (F_T/M_T)[u_{30}' + \sum_{j=1}^{N} Q_j \, \phi_j'(0) - \alpha_y] \, . \tag{126k}$$

## 3.4 Transformation Required at Launch

Because different reference frames and mode shapes are used in describing the motion of the rocket during the launch and free-free phases, a rather complicated transformation is required at the instant of launch. Simply put, we must determine "initial" conditions on the free-flight variables using the "final" conditions on the launch variables. Here, of course, the instant of launch is the "final time for the launch phase and the initial time for the free-flight phase.

We first undertake the task of determining the orientation of the $Cu_1u_2u_3$ frame at launch. The inertial orientation of this frame is defined by the

Euler angles $\psi$, $\theta$ and $\phi$ in a 3-2-1 rotation sequence. Also, its orientation relative to the Pxyz frame is as a result of the fact that it is the centroidal, principal frame is defined by the two small angles $\mu_2$ and $\mu_3$ which must be found by using the equations,

$$\mu_2 = -\int_0^L \sigma(z_o+\zeta-z_C)(x-x_C)dx/I_T \tag{127a}$$

and

$$\mu_3 = \int_0^L \sigma(y_o+\eta-y_C)(x-x_C)dx/I_T \ , \tag{127b}$$

where $(x_C, y_C, z_C)$ is the location of the rocket center of mass in the Pxyz reference frame. The inertial orientation of the Pxyz reference frame at the instant of launch is defined by the angles $\Theta_L$ and $\Phi$. Thus, the inertial orientation of $Cu_1u_2u_3$ reference frame at the instant of launch can be specified using either $\Theta_L$, $\Phi$, $\mu_2$ and $\mu_3$, or the corresponding values of $\psi$, $\theta$ and $\phi$. By forming the rotation matrices which are associated with each of these sets of angles and equating certain elements, the following equations for $\psi$, $\theta$ and $\phi$ may be obtained:

$$\psi = \tan^{-1}\{(\mu_3 c\Phi + \mu_2 s\Phi)/[c\Theta_L+(\mu_3 \ s\Phi \ -\mu_2 c\Phi)s\Theta_L]\} \ , \tag{128a}$$

$$\theta = \sin^{-1}[s\Theta_L+(\mu_2 c\Phi-\mu_3 s\Phi)c\Theta_L] \tag{128b}$$

and

$$\phi = \tan^{-1}\{(-\mu_3 \ s\Theta_L + s\Phi c\Theta_L)/(-\mu_2 s\Theta_L + c\Phi c\Theta_L)\}. \tag{128c}$$

The angular velocity of the $Cu_1u_2u_3$ of $\underline{\omega}$ are related to $\Omega_x$, $\Omega_y$ and $\Omega_z$ through the approximate equations,

$$\omega_1 \simeq \Omega_x \quad , \tag{129a}$$

$$\omega_2 \simeq \dot{\mu}_2 - \mu_3\Omega_x \tag{129b}$$

and

$$\omega_3 \simeq \dot{\mu}_3 + \mu_2\Omega_x ,$$

which are approximate only in that $\mu_2$ and $\mu_3$ are assumed to be very small angles and $\dot{\mu}_2$ and $\dot{\mu}_3$ are also assumed to be reasonably small.

Further, the location of the center of mass C with respect to the fixed OXYZ frame and its velocity at launch are needed. Letting $X_C$, $Y_C$ and $Z_C$ denote the inertial coordinates of C,

$$\begin{bmatrix} X_C \\ Y_C \\ Z_C \end{bmatrix} = \begin{bmatrix} c\Theta_L & 0 & s\Theta_L \\ 0 & 1 & 0 \\ -s\Theta_L & 0 & c\Theta_L \end{bmatrix} \begin{bmatrix} 1 & 0 & 0 \\ 0 & c\Phi & -s\Phi \\ 0 & s\Phi & c\Phi \end{bmatrix} \begin{bmatrix} x_{L_C} \\ y_C \\ z_C \end{bmatrix} ,$$

where $x_{L_C} = x_{L_P} + x_C$ and $x_{L_P}$ in the $x_L$-coordinate of point P. Moreover, the $u_j$-components of the velocity of the center of mass are, up to launch,

$$u = \dot{x}_{L_P} \quad , \tag{131a}$$

$$v = -\mu_3 u + \dot{y}_C - \Omega_x z_C \tag{131b}$$

and

$$w = \mu_2 u + \dot{z}_C + \Omega_x y_C . \tag{131c}$$

Finally, the new generalized coordinates, or mode shape amplitudes, and the first time derivatives can be found by using the following equations:

$$\underline{P} = -\mu_{3b}\,\underline{s} + \underline{\underline{T}}\,\underline{p} - y_{Cb}\,\underline{r} \quad , \tag{132a}$$

$$\underline{Q} = \mu_{2b}\,\underline{s} + \underline{\underline{T}}\,\underline{q} - z_{Cb}\,\underline{r} \quad , \tag{132b}$$

$$\dot{\underline{P}} = -\dot{\mu}_{3b}\,\underline{s} + \underline{\underline{T}}\,\dot{\underline{p}} - \dot{y}_{Cb}\,\underline{r} \quad , \tag{132c}$$

and

$$\dot{\underline{Q}} = \dot{\mu}_{2b}\,\underline{s} + \underline{\underline{T}}\,\dot{\underline{q}} - \dot{z}_{Cb}\,\underline{r} \quad , \tag{132d}$$

where

$$\mu_{2b} = -\underline{\ell}^T\,\underline{p}/I_T \quad , \tag{133a}$$

$$\mu_{3b} = \underline{\ell}^T\,\underline{q}/I_T \quad , \tag{133b}$$

$$y_{Cb} = \underline{m}^T\,\underline{p}/M_T \quad , \tag{133c}$$

$$z_{Cb} = \underline{m}^T\,\underline{q}/M_T \quad , \tag{133d}$$

$$\underline{s} = \int_0^L (x-x_C)\underline{\phi}\,dx \quad , \tag{133e}$$

$$\underline{\phi} = (\phi_1\ \phi_2\ \ldots\phi_N)^T \quad , \tag{133f}$$

$$\underline{r} = \int_0^L \underline{\phi}\,dx \tag{133g}$$

and the elements of $\underline{\underline{T}}$ are

$$t_{ij} = \int_0^L \psi_i\phi_j\,dx \quad (i,j=1,2,\ldots,N). \tag{133h}$$

Equations (132a) and (132b) were obtained by setting

$$u_{2e} = - \mu_{3e}(x-x_c) + \eta \tag{134a}$$

$$u_{3e} = \mu_{2e}(x-x_c) + \zeta \tag{134b}$$

using Eqs. (104) and (124), multiplying each of Eqs. (134) by $\phi_i$ successively with $i = 1,2,\ldots,N$ and integrating over the length of the rocket. In Eqs. (134), $\mu_{2e}$ and $\mu_{3e}$ are the principal axes rotations due to bending only. Equations (132c) and (132d) were obtained from

$$\dot{u}_{2e} = - \dot{\mu}_{3e}(x-x_c) + \dot{\eta} \tag{135a}$$

and

$$\dot{u}_{3e} = \dot{\mu}_{2e}(x-x_c) + \dot{\zeta} \tag{135b}$$

using the same method as above.

## 3.5 Comments on Simulation

The approximate, ordinary differential equations for the launch phase and the free-flight phase as well as the necessary transformation equations form the basis for a computer program which was developed during the latter stages of this study. The program is intended to be used in studying the effects of various factors, such as placement of the supports for a rocket, on the motion of the rocket. It was hoped that this program would be sufficiently operational in time to compare results from it with those from the two-body rocket model program. However, the program is not yet to the stage that we wish to publish results obtained using it.

From the preliminary results thus far obtained, it appears that the continuous model program produces numerical values of the right orders of magnitude for the constrained (on-launcher) motions of a uniform rocket model. Also, realistic "launch" values, which indicate that due to its bent shape at launch the rocket's principal axes have nonzero angular rates, have been computed.

## SECTION 4. CONCLUSIONS AND RECOMMENDATIONS

### 4.1 Conclusions

The two-body model of a flexible free-flight rocket yields results for angular motion of the nose of such a rocket which agree very well with results derived from optical lever data. To achieve agreement in the case considered, mechanical thrust misalignment was introduced into the model to produce oscillations in the time histories of the yaw and pitch of the rocket's nose with a frequency close to the spin frequency. Dynamic mass imbalance of an equivalent amount would have produced the same results.

The very good agreement between theory and experiment indicates that the model is both qualitatively and quantitatively valid. This in turn supports the conclusion that the transverse bending of a free-flight rocket can result in significant transverse rates at launch. As an example, for the GEM #7 model, a one-milliradian deflection angle of the nose of the rocket model results in a transverse "steady-state" rate of 0.00816 rad/sec. Furthermore, a one-milliradian per second angular rate of the nose of that model results in a transverse "steady-state" rate of 0.000322 rad/sec. When consideration is given to the fact that the angular rates due to bending may be as large as 0.4 rad/sec, it is seen that "steady-state" transverse rates of free-flight rockets in excess of 0.1 rad/sec (≈ 100 mils/sec) may result from transverse bending.

The magnitude of the "steady-state" transverse rate predicted by the two-body model depends significantly upon the location of a rocket's support points (see Table 2).

Although the presence of rather severe transverse bending of free-flight rockets has been documented[12] the results obtained from the two-body model for

on-launcher motion indicate that gravity and thrust effects alone do not cause very large deflections of the nose of the free-flight rocket modeled. Hence, the cause, or causes, of deflections on the order of one-half to one milliradian, which have been observed, are still not known.

As far as the continuous rocket model is concerned, the results obtained thus far are incomplete. However, the use of two different types of mode shapes appears to promise significant improvement over the use of a single type, because the transition from constrained to unconstrained motion is modeled in a much more realistic manner.

## 4.2 Recommendations

The following recommendations are based on the results of this study.

1. Because transverse bending of a free-flight rocket can result in significant transverse rates of the rocket as a whole ("rigid body" rates) subsequent to launch, a concerted effort should be made to determine the cause, or causes, of bending other than gravity and thrust (as it was modeled herein). A by-product of such an effort should be methods for reducing transverse bending and/or designing rockets and launchers which minimize the "rigid-body" rotation rates caused thereby.

2. The two-body model computer program should be used in other attempts to duplicate the optical-lever-derived pitch and yaw time histories of free-flight rockets. This would provide additional input as to the exactness of the model and also lead to a better understanding of the problem in general.

3. The continuous rocket model program should be used in the same manner as the two-body one with the primary objective of comparing the results obtained from the two programs.

4. Aerodynamic forces and moments, and possibly time varying inertia properties, should be introduced into the two-body and continuous models used for the free-flight phase. This would allow simulation of the rocket from launch to impact. Hence, the way in which transverse bending affects entire trajectories could be determined.

## REFERENCES


1. Free Flight Rocket Workshop, June 14-18, 1976, U.S. Army Missile Command, Redstone Arsenal, Alabama.

2. Cochran, J. E., Jr., "Investigation of Factors which Contribute to Mallaunch of Free Rockets," Final Report on U.S. Army Grant DAHC04-75-0034, Engineering Experiment Station, Auburn University, Auburn, Alabama, January 1976.

3. Beal, T. R., "Dynamic Stability of a Flexible Missile under Constant and Pulsating Thrusts," AIAA Journal, Vol. 3, No. 3, March 1965, pp. 486-495.

4. Wu, J. J., "Missile Stability Using Finite Elements - An Unconstrained Variational Approach," AIAA Journal, Vol. 14, No. 3, March 1976, pp. 313-319.

5. Meirovitch, L., and Wesley, D. A., "On the Dynamic Characteristics of a Variable-Mass Slender, Elastic Body under High Acceleration," AIAA Journal, Vol. 5, No. 8, August, 1967, pp. 1439-1447.

6. Reis, G. E., and Sundberg, W. D., "Calculated Aeroelastic Bending of a Sounding Rocket Based on Flight Data," Journal of Spacecraft and Rockets, Vol. 4, No. 11, November 1967, pp. 1489-1494.

7. Womack, W. C., Bert, C. W., and P rdreauville, F. J., "Dynamics of Sounding Rockets at Burnout," Journal of Spacecraft and Rockets, Vol. 11, No. 10, October 1974, pp. 716-720.

8. Meirovitch, L., "General Motion of a Variable-Mass Flexible Rocket with Internal Flow," Journal of Spacecraft and Rockets, Vol. 7, No. 2, February 1970, pp. 186-195.

9. Cochran, J. E., Jr., Batson, J. L., Jr., and Christensen, D. E., "Dynamic Coupling of Gross and Fine Motions of a Flexible Spinning Free Rocket," AIAA Paper No. 77-1141, Presented at the AIAA Atmospheric Flight Dynamics Conference, Hollywood, Florida, August 8-10, 1977.

10. Bisplinghoff, R. L., Ashley, H., and Holfmann, R. L., Aeroelasticity, Addison-Wesley Publishing Company, Inc., Reading, Mass., 1955, Chapters 3 and 4.

11. Likins, P. W., "Effects of Energy Dissipation on the Free Body Motions of Spacecraft," Technical Report No. 32-860, Jet Propulsion Laboratory, California Institute of Technology, Pasadena, California, July 1, 1966.

12. Anonymous, "Free Flight Rocket Firing GEM #7," U.S. Army Missile Research and Development Command, Redstone Arsenal, Alabama, February 5, 1976.

## APPENDIX A

## DEFINITION OF THE INTERNAL FORCE

The internal force component f(x) in the rocket is assumed to be due to the action of a force with the magnitude of the thrust acting at the head end of the rocket motor as shown in Fig. A.1. Since no aerodynamic forces are considered, the only other forces acting on the rocket are the force due to gravity and a transverse force at P which is due to the turning of the fluid flow from the rocket motor by a mechanically misaligned nozzle and a bent rocket. Letting $M_T$ denote the total mass of the rocket and $\Theta_L$ the launcher elevation angle,

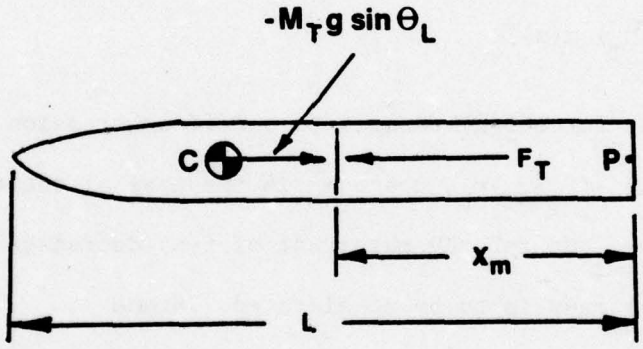


Fig. A.1. Simplified model for determining f(x).

the x-component of the force on the rocket is $-M_T g \sin \Theta_L$ during the launch phase and, during the part of the free-flight phase of interest here, it has essentially this value because the pitch and yaw angles remain small, if we do not consider catastrophic launches. Also, due to the small angular rates and transverse velocity components the acceleration of each part of the rocket in the x-direction is approximately $F_T/M_T - g \sin \Theta_L$.

The internal force at a value of x less than $x_M$ must be a tension force and so is positive using our chosen sign convention. This force must be of sufficient magnitude to impart, with the help of gravity, to the part of the rocket aft of its location the acceleration stated above. Thus, since the mass accelerated is

$$m(x) = \int_0^x \sigma \, dx, \quad 0 \leq x < x_m, \tag{A-1}$$

$$+ f(x) - m(x)\, g \sin \Theta_L = m(x)\, (F_T/M_T - g \sin \Theta_L), \tag{A-2}$$

or

$$f(x) = (F_T/M_T)\, m(x). \tag{A-3}$$

At $x=x_{M_+}$, the force $f(x)$ changes to one of compression. At $x=x_{M_+}$ it must have the magnitude $-(F_T/M_T)m_N$, where $m_N$ is the mass of the rocket's nose section. From $x=x_{M_+}$ to $x=L$ the magnitude of $f(x)$ decreases because, with increasing x, less mass is to be accelerated. Since

$$m_N = \int_{x_M}^{L} \sigma \, dx \tag{A-4}$$

and since the mass accelerated by $f(x)$ for $x_M < x \leq L$ is

$$m(x) = m_N - \int_{x_M}^{x} \sigma \, dx \, , \tag{A-5}$$

it follows that for $x \geq x_{M_+}$,

$$f(x) = -(F_T/M_T)[m_N - \int_{x_{M_+}}^{x} \sigma \, dx] \, . \tag{A-6}$$

For the special case of constant masses per length $\sigma_M$ for the motor and $\sigma_N$ for the nose,

$$f(x) = -(F_T/M_T)\,\sigma_M\,x \quad , \quad 0 \le x < x_{M_-} \tag{A-7a}$$

$$f(x) = (F_T/M_T)(L-x)\sigma_N \quad , \quad x_{M_+} < x \le L. \tag{A-7b}$$

It is clear from Eqs. (A-3) and (A-6) that $f(x_{M_-}) = F_T\, m_M/M_T$ and $f(x_{M_+}) = -F_T m_N/M_T$, while f(0) and f(L) are zero. Thus,

$$\int_0^{x_{M_-}} \partial f/\partial x\, dx + \int_{x_{M_+}}^{L} \partial f/\partial x\, dx = F_T \, . \tag{A-8}$$

The force $\underline{f}(x)$ is <u>defined</u> as

$$\underline{f}(x) \triangleq f(x)\hat{\underline{i}} + F_T\left( (\theta_{3p} + \alpha_z)\hat{\underline{j}} + (\theta_{2p} - \alpha_y)\hat{\underline{k}}\right)\delta(x-0)$$

where $\delta(o)$ is the Dirac delta function and is zero for all x except x=0 and is 1 at that value of x, $\alpha_y$ and $\alpha_z$ are mechanical thrust misalignment angles and $\theta_{2p}$ and $\theta_{3p}$ are angles of rotation of the aft end of the rocket due to bending. For the free-flight phase, the unit vector $\hat{\underline{i}}$, $\hat{\underline{j}}$ and $\hat{\underline{k}}$ are replaced by $\hat{\underline{u}}_1$, $\hat{\underline{u}}_2$ and $\hat{\underline{u}}_3$, respectively.

## APPENDIX B

## MODE SHAPES FOR THE LAUNCH PHASE

The mode shapes used to approximate the transverse deflections of the continuous rocket model during the launch phase are those for a slender, uniform beam which is pinned at one end, point P, and at an arbitrary point Q as shown in Fig. B.1. The forward end is free.

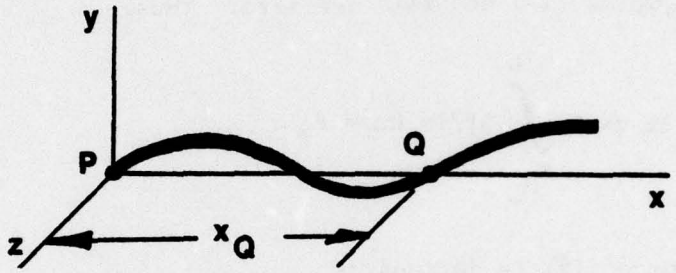


Letting EI denote the bending stiffness of the beam, $\sigma$ its mass per unit length, and L its length, the equation governing its transverse free vibration is

$$\sigma \ddot{y} = - EIy^{IV} \quad , \tag{B-1}$$

subject to the boundary conditions,

$$y(0,t) = 0 \quad , \tag{B-2a}$$

$$y''(0,t) = 0 \quad , \tag{B-2b}$$

$$y(x_Q,t) = 0 \quad , \tag{B-2c}$$

$$y''(L,t) = 0 \tag{B-2d}$$

and

$$y'''(L,t) = 0 \tag{B-2e}$$

and the continuity condition,

$$y'(x_{Q-},t) = y'(x_{Q+},t) \quad . \tag{B-3}$$

By using the usual method of separation of variables whereby we set

$$y = T(t)\, Y(x) \tag{B-4}$$

we get the two ordinary differential equations,

$$\ddot{T} = -\beta^4 (EI/\sigma) T \tag{B-5a}$$

and

$$Y^{IV} = \beta^4 Y \quad , \tag{B-5b}$$

where $\beta$ is a separation constant which must of course have only certain values, as determined by the boundary conditions (B-2) and the continuity condition (B-3).

The general solution to Eq. (B-5b) has the form,

$$Y = A \cosh \beta x + B \sinh \beta x + C \cos \beta x + D \sin \beta x \tag{B-6}$$

and the conditions (B-2), except the slope continuity conditions, can be used to obtain two functions $Y_1$ and $Y_2$ which satisfy those conditions. Explicitly,

$$Y_1 = \sin\bar{x}_Q [(\sin\bar{\beta}\bar{x})/\sin\bar{\beta}x_Q - (\sinh\bar{\beta}\bar{x})/\sinh\bar{\beta}\bar{x}_Q] \tag{B-7a}$$

and

$$Y_2 = f(\bar{x}_Q)/h(\bar{x}_Q)\{[\sin \bar{\beta}(1-\bar{x}) + \sinh \bar{\beta}(1-\bar{x})]/[\sin \bar{\beta}\alpha + \sinh \bar{\beta}\alpha]$$

$$-[\cos \beta(1-\bar{x}) + \cosh \beta(1-\bar{x})]/[\cos \bar{\beta}\alpha + \cosh \bar{\beta}\alpha] \ , \tag{B-7b}$$

where $\bar{\beta}=\beta L$, $\bar{x}=x/L$,

## APPENDIX C

## MODE SHAPES FOR THE FREE-FLIGHT PHASE

The equations which govern the transverse, vibrational motion of a free-free, slender uniform beam is, of course, the same as that given in Appendix B, namely,

$$\sigma\ddot{y} = EIy^{IV} , \tag{C-1}$$

where again $\sigma$ is the mass per unit length, $y=y(x,t)$ is the transverse displacement at x, EI is the bending stiffness, $(\dot{})=\partial(\ )/\partial t$ and $(\ )^{IV} = \partial^4(\ )/\partial x^4$. However, the boundary conditions Eq. (C-1) are, for a beam of length L,

$$y'''(0,t) = 0 , \tag{C-2a}$$

$$y^{IV}(0,t) = 0 , \tag{C-2b}$$

$$y'''(L,t) = 0 \tag{C-2c}$$

and

$$y^{IV}(L,t) = 0 . \tag{C-2d}$$

By setting $y = T(t)\ Y(x)$, and separating variables in Eq. (C-1), an equation for Y(x) can be found. Then, by using the boundary conditions (C-2) the solution,

$$Y(x) = (\cos \bar{\beta} - \cosh \bar{\beta})(\sin \bar{\bar{\beta}}x + \sinh \bar{\bar{\beta}}x)$$

$$-(\sin \bar{\beta} - \sinh \bar{\beta})(\cos \bar{\bar{\beta}}x + \cosh \bar{\bar{\beta}}x), \tag{C-3}$$

$$g(\bar{x}_Q) = \sin \bar{\beta}\bar{x}_Q(\sin \bar{\beta}\alpha + \sinh \bar{\beta}\alpha)(\cos \bar{\beta}\alpha + \cosh \bar{\beta}\alpha), \tag{B-8a}$$

$$h(\bar{x}_Q)=\sin \bar{\beta}\alpha \cosh \bar{\beta}\alpha - \cos \bar{\beta}\alpha \sinh \bar{\beta}\alpha \tag{B-8b}$$

and $\alpha = 1-\bar{x}_Q$.

The continuity of the slope of the beam at $x=x_Q$ requires that the eigenvalue $\beta$ satisfy the transcendental equation,

$$2(1+\cos \bar{\beta}\alpha \cosh \bar{\beta}\alpha)/(\sin \bar{\beta}\alpha \cosh \bar{\beta}\alpha -\cos \bar{\beta}\alpha \sinh \bar{\beta}\alpha)$$

$$= \coth \bar{\beta}\bar{x}_Q - \cot \bar{\beta}\bar{x}_Q \ . \tag{B-9}$$

We let $\bar{\beta}_j$, $j=1,2,\ldots$, denote values of $\bar{\beta}$ which satisfy Eq. (B-9) for a given value of $\alpha$. Then, the <u>normalized</u> mode shapes $\psi_j$ are defined by

$$\psi_j \triangleq \begin{cases} Y_1(x;\beta_j)/E_j \ , & 0 \le \bar{x} \le \bar{x}_Q \\ Y_2(x;\beta_j)/E_j \ , & \bar{x}_Q \le \bar{x} \le 1 \end{cases} \tag{B-10}$$

where

$$E_j^2 = \int_0^{x_Q} \sigma Y_1^{\,2}(x;\beta_j)dx + \int_{x_Q}^{L} \sigma\, Y_2(x;\beta_j)dx \ . \tag{B-11}$$

where $\bar{x} = x/L$, $\bar{\beta} = \beta L$ and the eigenvalue $\beta$ must satisfy the transcendental equation,

$$\cos \bar{\beta} \cosh \bar{\beta} = 1 \quad , \tag{C-4}$$

may be obtained.

We require here only the bending mode shapes, i.e., the rigid body mode shapes corresponding to $\beta = \beta_j = 0$, $j=0,1$, are not used. The normalized mode shapes used in the continuous model of the rocket are

$$\phi_j = Y(x,\beta_{j+1})/E_{j+1} \qquad (j=1,2,\ldots), \tag{C-5}$$

where

$$E_{j+1} = \int_0^L \sigma Y^2(x,\beta_{j+1})dx \quad . \tag{C-6}$$

# DISTRIBUTION

| | No. of Copies |
|---|---|
| Defense Documentation Center<br>Cameron Station<br>Alexandria, VA 22314 | 2 |
| Commander<br>US Army Missile R&D Command | |
| Attn: DRDMI-C | 3 |
| DRCMI-TLH, Mr. Christensen | 7 |
| DRDMI-ICBB, Mr. Edwards | 1 |
| DRDMI-TI | 2 |
| DRDMI-TBD | 2 |
| DRSMI-LP | 1 |
| Redstone Arsenal, AL 35809 | |
| Office of Naval Research<br>Atlanta Area Office<br>Attn: Mr. Henry Cassall<br>Georgia Institute of Technology<br>325 Hinman Research Bldg.<br>Atlanta, GA 30332 | 1 |

# SUPPLEMENTARY

# INFORMATION

DEPARTMENT OF THE ARMY
UNITED STATES ARMY MISSILE COMMAND
REDSTONE ARSENAL, ALABAMA 35809

AD-A061109

DRSMI-TI(R&D) 24 July 1979

SUBJECT: Errata for Technical Report T-CR-78-21, subject: EFFECTS OF TRANSVERSE BENDING ON THE MOTION OF FREE-FLIGHT ROCKETS, dated September 1978

TO: Recipients of Subject Report

The following changes should be made to subject report:

Page 4, second paragraph, third line: "P" should be "$C_1$."

Page 20, Eq. (38): "$\underline{\underline{I}}$" should be "$\underline{\underline{I}}_1$."

Page 24, first line: Delete "negatives of the."

Page 24, Eq. (48) should read: $\underline{x}_h(t) = \underline{\underline{E}}\ \underline{\underline{D}}\ \underline{\underline{E}}^{-1}\ \underline{x}_o$ .

Page 26, Eq. (55): "$\underline{\underline{P}}(\tau)$" should be "$\underline{\underline{P}}_i(\tau)$" and "$\underline{\underline{Q}}(\tau)$" should be "$\underline{\underline{Q}}_i(\tau)$."

Page 26, Eq. (56): "$\underline{\underline{P}}(\tau)$" should be "$\underline{\underline{P}}_i(\tau)$" and and the [ ]'s on the (2,2) element of $\underline{\underline{P}}_i(\tau)$ should be deleted.

Page 27, second line from bottom: "sin +" should be "sin $\Phi$ +."

Page 28, tenth line: "positive" should be "negative."

Page 28, eighteenth line: "...apply to..." should be "...apply, and..." and ...quasi rigid,..." should be "...quasi-rigid,..."

Page 28, footnote: Add "and their displacements relative to the main part of the spacecraft are small."

Page 32, seventh line: Second "[" should be "(."
ninth and tenth lines: Delete "(" before "d."
thirteenth line: "$\Psi_o$" should be "$\Theta_o$."
fifteenth line: "$\Theta_o$" should be "$\Psi_o$."

Page 41, Table 4: Units of k should be "(Nt/m)."

DRSMI-TI(R&D) 24 July 1979

SUBJECT: Errata for Technical Report T-CR-78-21, subject: EFFECTS OF TRANSVERSE BENDING ON THE MOTION OF FREE-FLIGHT ROCKETS, dated September 1978

Page 71, thirteenth line: Delete first "P" within brackets.

Page 76, third line: Delete "is."

Page 77, first line: Change to read: "The $u_1$, $u_2$ and $u_3$ components of $\underline{\omega}$ are related to $\Omega_x$, $\mu_2$, $\mu_3$, $\dot{\mu}_2$ and $\dot{\mu}_3$ as,"

sixth line: Add equation number (129c).

second paragraph: Add equation number (130).

second paragraph, seventh line: "in" should be "is."

Page 79: Equations (134a) and (134b) should read:

$$u_{2e} = -\mu_{3b}(x-x_C) + \eta - y_{Cb}$$

$$u_{3e} = -\mu_{2b}(x-x_C) + \zeta - z_{Cb} ,$$

Page 79, sixth line: "$\mu_{2e}$ and $\mu_{3e}$" should read "$\mu_{2b}$ and $\mu_{3b}$."

Page 79: Equations (135a) and (135b) should read:

$$\dot{u}_{2e} = -\dot{\mu}_{3b}(x-x_C) + \dot{\eta} - \dot{y}_{Cb}$$

and

$$\dot{u}_{3e} = \dot{\mu}_{2b}(x-x_C) + \dot{\zeta} - \dot{z}_{Cb} ,$$

John W. Chambers

JOHN W. CHAMBERS
Chief, Technical Information Office
Technology Laboratory